Cancer Letters 449 (2019) 237–251

Contents lists available at ScienceDirect

Cancer Letters

journal homepage: www.elsevier.com/locate/canlet

Original Articles

Oncogenic PITX2 facilitates tumor cell drug resistance by inverse regulation of hOCT3/SLC22A3 and ABC drug transporters in colon and kidney cancers

Wing-Kee Lee*, Frank Thévenod

Institute of Physiology, Pathophysiology and Toxicology, Centre of Biomedical Education and Research (ZBAF), Witten/Herdecke University, Stockumer Strasse 12, Witten, Germany

ARTICLE INFO

Keywords:
ATP binding cassette
Chemoresistance
Transcription factor
Developmental pathways in cancer
Organic cation transporter
Homeobox

ABSTRACT

Oncogenic pituitary homeobox 2 (PITX2), a de facto master regulator of developmental organ asymmetry, previously upregulated multidrug resistance (MDR) P-glycoprotein ABCB1 in A498 renal cell carcinoma (RCC) cells. The role of PITX2 isoforms in MDR cancers was investigated. Data mining correlated elevated *PITX2* in > 30% of cancers analyzed, maximally in colon (4.4-fold), confirmed in co-immunostaining of colon and renal cancer microarrays wherein ABCB1 concomitantly increased in RCC. Drug-resistant colorectal adenocarcinoma Colo320DM cells exhibited increased nuclear PITX2 (40-fold), *PITX2* promoter activity (27-fold) and *ABCB1* (8000-fold) compared to drug-sensitive Colo205. ABCB1 inhibitor PSC833/valspodar or *PITX2* siRNA reversed doxorubicin resistance. Nuclei from Colo320DM and A498 cells harbored PITX2A/B1 and PITX2A/B1/B2/Cα/Cβ, respectively. ChIP-qPCR evidenced PITX2 promoter binding in drug exporters *ABCB1*, *ABCC1*, *ABCG2* and importer hOCT3/*SLC22A3*. In A498, 786-O, Caki-1, Colo320DM, and Caco2 cells, *PITX2* siRNA diminished exporters, increased hOCT3/*SLC22A3* expression and activity, and reverted vincristine resistance. Heterologous PITX2 expression induced ABCB1, repressed hOCT3/SLC22A3, enhanced vincristine resistance and diminished proliferation inhibition wherein PITX2A and PITX2C were most effective. Furthermore, PITX2 activity and MDR depended on phosphorylation by GSK3 in A498 cells. Conclusively, oncogenic PITX2 limits sensitizing drug uptake and potentiates cytoprotective drug efflux, contributing to MDR phenotype.

1. Introduction

Pituitary homeobox 2/paired-like homeodomain transcription factor 2 (PITX2) is a bicoid class homeodomain protein with essential roles in embryonic development, including organ asymmetry [12], as evidenced by embryonic lethality in *PITX2* knockout mice [30]. The PITX2 isoforms PITX2A, PITX2B and PITX2C, and their splice variants [26], transcriptionally regulate isoform-specific target genes in development and cellular functions. For example, PITX2A alters cytoskeleton and migration [46], PITX2B regulates heart asymmetry [18], and PITX2C activates atrial natriuretic factor in cardiogenesis [13]. Conversely, PITX2D lacks a functional homeodomain and hence does not bind DNA. In fact, PITX2D suppresses transcriptional activity of PITX2A and PITX2C through direct protein-protein interactions [5]. In adults, PITX2 activity is restricted to selective tissues [4,43].

Developmental signaling pathways, such as Wnt, Hippo and Notch, are frequently reactivated during carcinogenesis [42]. Early studies linked PITX2 to Wnt/β-catenin signaling [23]. Subsequently, direct evidence for regulation of cell cycle control genes (cyclin D2 [23], cyclin D1 and c-Myc [2]), cyclin D2 in thyroid cancer [22] and cyclin A1 in papillary thyroid carcinoma [31] by PITX2 paved the way for its role in cancer. Though increased PITX2 has been associated with cancer progression in various tumors [3,11,20], the subset of genes regulated by PITX2 appears to be cancer type-specific as decreased PITX2 has also been reported in pancreatic [44] and cervical [45] cancers, highlighting the necessity to understand cancer-specific deregulated oncogenic PITX2.

ATP-binding cassette (ABC) transporters, such as multidrug resistance (MDR) P-glycoprotein MDR1/*ABCB1,* multidrug resistance related protein MRP1/*ABCC1*, and breast cancer resistance protein 2

Abbreviations: ABC, ATP-binding cassette; APC, adenomatous polyposis coli; CSC, cancer stem cell; DOX, doxorubicin; EMT, epithelial-to-mesenchymal transition; GENT, Gene Expression across Normal and Tumor tissue; GEO, gene expression omnibus; hOCT3, human organic cation transporter 3; HPCT, human proximal convoluted tubule; MDR, multidrug resistance; Nuc, nuclear; PITX2, pituitary homeobox 2; PNS, postnuclear supernatant; RCC, renal cell carcinoma; SLC, solute carrier; TMA, tissue microarray; VIN, vincristine

* Corresponding author. Institute of Physiology, Pathophysiology and Toxicology, Witten/Herdecke University, 58453, Witten, Germany.
E-mail addresses: wing-kee.lee@uni-wh.de (W.-K. Lee), frank.thevenod@uni-wh.de (F. Thévenod).

https://doi.org/10.1016/j.canlet.2019.01.044
Received 26 September 2018; Received in revised form 25 January 2019; Accepted 29 January 2019
0304-3835/ © 2019 Elsevier B.V. All rights reserved.

BRCP2/*ABCG2*, are physiologically expressed at barrier sites, including colon, liver, kidney and blood-brain barrier, where they serve to protect against xenobiotics and toxic metabolites [14] and are predominantly governed by transcription factors (reviewed in Ref. [38]). Aberrantly upregulated *ABCB1* in tumor cells prevents chemotherapeutic drugs from reaching their intracellular destination by extrusion across the plasma membrane [1] or sequestration into acidic vesicles [47] and, together with other drug transporters, represents a major hurdle in successful treatment of chemo-resistant cancers [29,41]. Furthermore, drug entry pathways contribute to sensitization of tumors to chemotherapy. To this end, the solute carrier (SLC) family of organic cation and anion transporters (OCTs, OATs; SLC22A subfamily) has received attention. Downregulation of hOCT3/*SLC22A3*, which is broadly expressed and transports vinca alkaloids, such as vincristine, has been observed in patients with liver [17], prostate [15], head and neck [21] and esophageal [10] cancers.

We recently reported ABCB1 as a PITX2 target gene [27]. However, PITX2 isoform-specific regulation of drug transporters closely linked to MDR has not been addressed. In this study, we report for the first time PITX2 association in *ABCC1*, *ABCG2*, *ABCB1* and hOCT3/*SLC22A3* promoters, inverse regulation of drug importers and exporters that are mechanistically linked to MDR and distinct PITX2 isoform function in colon and kidney cancer cells.

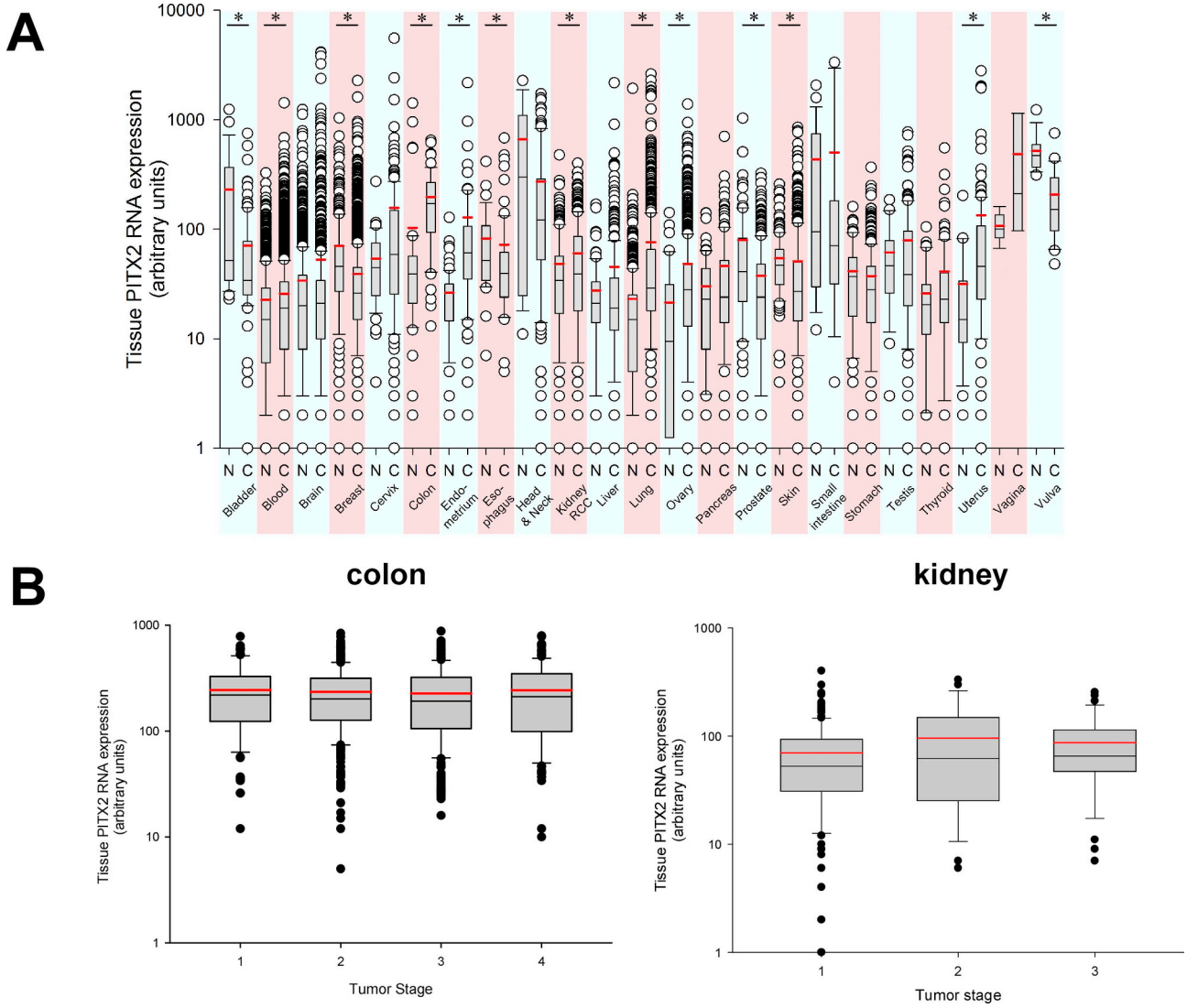

Fig. 1. PITX2 expression is elevated in human colon and kidney cancers. (A) *In silico* analysis of *PITX2* RNA expression in human cancers [C] compared to normal tissue [N] using data available from genome-wide microarrays. Box plots mark the 25th to 75th percentiles and whisker error bars indicate the 10th and 90th percentiles. Symbols represent outliers. Median is indicated by the line within the box and mean is indicated by red lines. RCC = renal cell carcinoma. Nonparametric analyses using Mann-Whitney *U* test reported significantly increased *PITX2*. (B) Comparison of *PITX2* expression in tumors at different stages. Box and whisker plots are as described above. Cancer tissue microarrays (TMAs) from colon adenocarcinomas (C) and kidney carcinomas (D) were immunostained for PITX2 and nuclei were counterstained with Hoechst to identify single cells (inset). Parallel samples without primary antibody served as negative controls. Images are representative of three individual experiments. Scale bar = 10 µm. Arrows indicate nuclear presence of PITX2. Percentage of cells exhibiting positive nuclear PITX2 (PITX2$_{nuc}^{+}$) were quantified in colon and kidney cancer subtypes. Statistical analyses using one-way ANOVA compare cancer adjacent normal tissue and cancer subtypes to normal renal or colon tissue. (E) Drug-sensitive Colo205 and drug-resistant Colo320DM were immunostained for PITX2 after fixation and permeabilization (scale bar = 20 µm). Nuclei were counterstained with Hoechst. Fluorescence intensity was quantified by threshold analysis and normalized to cell number (n = 5). (F) Colocalization analysis between PITX2 and Hoechst indicate nuclear presence in Colo320DM. (G) Luciferase reporter gene assay for *PITX2* promoter activity in Colo205 and Colo320DM cells transfected with empty vector or *PITX2-Luc* (n = 7–9). Relative luminescence units per mg protein in empty vector-transfected cells: Colo205, 1.32 ± 0.93; Colo320DM, 0.01 ± 0.01. Pairwise comparisons were performed using unpaired Student's t-test. *p < 0.05, **p < 0.01, ***p < 0.001. (For interpretation of the references to color in this figure legend, the reader is referred to the Web version of this article.)

2. Materials and methods

2.1. Microarray data

Data mining analysis of gene expression patterns in normal and human cancer tissues was performed using the freely accessible database GENT (Gene Expression across Normal and Tumor Tissue, http://mgrc.kribb.re.kr/GENT) [39]. Comparative datasets were compiled from 479 data series using GeneChip Human Genome Microarray platforms (U133A and U133 Plus 2.0, Affymetrix) (Supplementary Table 1). Tumor pathology data, where available, were extracted from Gene Expression Omnibus (GEO) public repository.

2.2. Cell culture, treatments and transient transfections

Human renal carcinoma (A498, ACHN) [27] and colon adenocarcinoma (Colo320DM, Colo205, SW480) cell lines were purchased from Cell Lines Service, authenticated by short-tandem repeats profiling and used for < 20 passages. Renal adenocarcinoma 786-O, renal clear cell carcinoma Caki-1 and colon adenocarcinoma Caco2 cells were purchased from ATCC. Cell culture reagents were from GibCo or Sigma-Aldrich. Colo320DM was maintained in Ham's F-12 nutrient mixture supplemented with 10% fetal bovine serum (FBS), 50 U/ml penicillin, 50 µg/ml streptomycin and 2 mM L-glutamine. Colo205 and SW480 cells were cultured in DMEM/F-12 supplemented with 5% FBS, 50 U/ml penicillin and 50 µg/ml streptomycin. Human kidney proximal tubule cells (HPCT) were kindly provided by Dr. Ulrich Hopfer (Case Western Reserve University) and cultured as described [35]. 786-O and Caki-1 cells were cultured in RPMI and McCoy's 5A basal media, respectively, supplemented with 10% FBS, 50 U/ml penicillin, and 50 µg/ml streptomycin. Caco2 cells were grown in DMEM:F12 (1:1), 10% FBS, 50 U/ml penicillin, 50 µg/ml streptomycin and 1.2 mg/ml $NaHCO_3$ medium. All cell lines were routinely tested for mycoplasma. Doxorubicin (DOX) and vincristine sulfate (VIN) were incubated in absence of serum. Ethidium bromide uptake experiments were performed as previously described [28].

Plasmids encoding mouse *Pitx2a* and *Pitx2b* were generously provided by Dr. D. Bernard (McGill University) and *Pitx2c* by Dr. B.A. Amendt (University of Iowa). Plasmids were transfected using Lipofectamine LTX Plus or Lipofectamine 2000 (Life Technologies) per manufacturer's instructions. $PITX2^{ABC}$ siRNA (EHU072181, Sigma-Aldrich) was transfected as previously described [27]. For proliferation, trypan blue and combined PITX2 isoform overexpression experiments, cells in 24-well plates were transfected with 0.3 µg total DNA using 0.75 µl transfection reagent per well.

2.3. Immunostaining of cancer tissue microarrays

Human colon (CO804a) and renal (T072a, KD804a) cancer tissue microarrays (TMAs) with pathological assessment (US Biomax) were deparaffinized and rehydrated. After antigen retrieval and blocking in 5% goat serum/PBS, primary antibodies against ABCB1 (UIC2, 1:100, sc-73354, Santa Cruz) and $PITX2^{ABC}$ (1:500, PA-1020, Capra Science) were incubated overnight at 4°C in a humidified chamber. Negative controls were incubated with blocking buffer alone. Species-specific fluorophore-coupled goat secondary antibodies were diluted 1:500. Nuclei were counterstained with 0.8 µg/ml Hoechst-33342 (Hoechst).

For immunohistochemistry, endogenous horseradish peroxidase and alkaline phosphatase were blocked with Bloxall (Vector Labs) following rehydration. Antigens were retrieved and ABCB1 (UIC2, 1:100) and

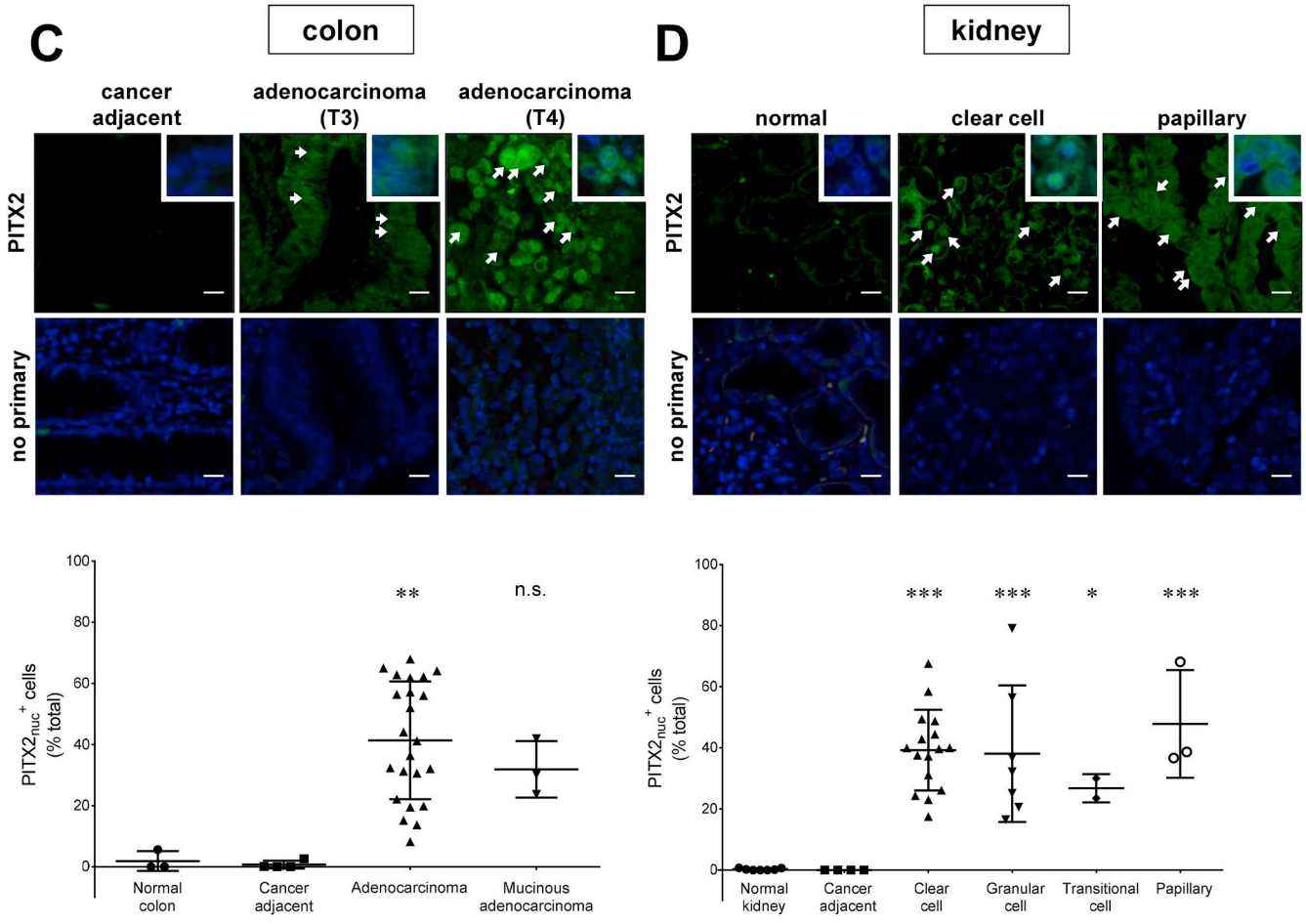

Fig. 1. (*continued*)

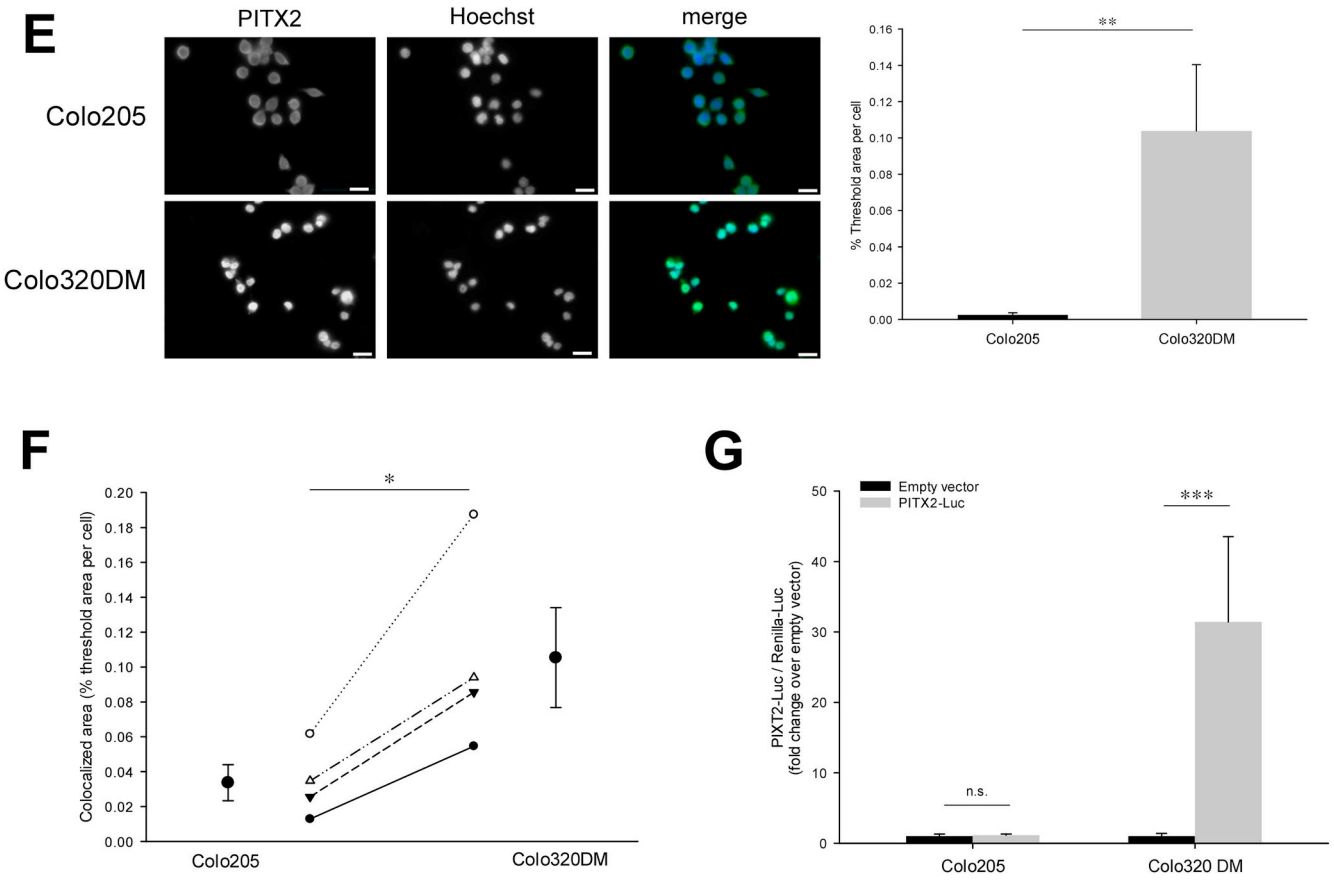

Fig. 1. (*continued*)

Table 1
Tumor stage and grade of PITX2 expressing human cancer tissues. Cancer tissue microarrays were stained for PITX2 by immunofluorescence. For kidney, 90 tissue cores were examined (T072a, KD804a) and for colon, 72 tissue cores were examined (CO804a). Tumor grade: 1 = well differentiated, 2 = moderately differentiated, 3 = poorly differentiated, 4 = undifferentiated. Tumor stage: I = small tumor and contained in organ, II = tumor is larger than in stage I with possible spread to lymph nodes close to tumor, III = tumor is larger than stage II with possible spread into surrounding tissues and lymph nodes, IV = tumor has metastasized. Tumor Node Metastasis (TNM) grading system: T1 = tumor invades submucosa, T2 = tumor invades muscularis propria, T3 = tumor invades through muscularis propria into subserosa or into non-peritonealized pericolic or perirectal tissues, T4 = tumor directly invades other organs or structures and/or perforates visceral peritoneum. N1 = metastasis in 1–3 regional lymph nodes, N2 = metastasis in 4 or more regional lymph nodes. M0 = no distant metastasis, M1 = distant metastasis.

		Colon		Kidney	
		Incidence	Percent	Incidence	Percent
Tumor Grade	1	6/25	24	12/38	31.6
	2	10/30	33.3	10/36	27.8
	3	9/13	69.2	1/2	50
	4	0/0	0	0/0	0
Tumor Stage	I	5/10	50	2/6	33.3
	II	11/37	29.7	5/8	62.5
	III	7/21	33.3	2/4	50
	IV	3/4	75	0/0	0
TNM Grading					
Primary tumor	T1	1/2	50	15/56	26.8
	T2	4/8	50	9/21	42.9
	T3	4/18	22.2	4/10	40
	T4	17/44	38.6	0/1	0
Metastasis	N1/N2	10/25	40	0/0	0
	M1	3/4	75	0/0	0

PITX2 (ab55599, Abcam, 1:500) were detected using MultiView Immunohistochemistry Kit (ADI-950-101-0001, Enzo Life Sciences).

Slides were digitalized using Mirax Scan (Zeiss) and quantification analyses were performed using FIJI/ImageJ [37] where tumor cells from five random areas were quantified independently by two assessors for $PITX2_{nuc}$ positive ($PITX2_{nuc}^{+}$) cells, ABCB1 positive ($ABCB1^{+}$) cells and were considered dual positive ($PITX2_{nuc}^{+}/ABCB1^{+}$) when > 40% $PITX2_{nuc}^{+}$ cells exhibited concomitant increase in ABCB1. Stroma and blood vessels were excluded.

2.4. Immunofluorescence staining of cell lines

Cell lines were immunostained and analyzed as previously described [27]. Colocalization analysis was performed using FIJI/Image J from thresholded binary images and percentage overlapping area was deduced using image calculator Boolean operation “AND”.

2.5. Luciferase reporter gene assay

PITX2 reporter gene assay has been described elsewhere [27]. Kinase inhibitors were added directly to cells 12 h posttransfection and incubated for a further 12 h prior to analysis.

2.6. Cell viability assays

Clonogenic survival and MTT assays were performed as previously described [27]. The survival fraction was derived from number of colonies/number of cells plated. For trypan blue exclusion, cells were diluted 1:2 with 0.4% trypan blue and automatically counted (Countess II FL, Thermo Fisher). In proliferation assays, 5000 cells were grown ≤18 days and stained with 6% glutaraldehyde/0.5% crystal violet. Plates were digitalized and % area occupied by cells was analyzed in

Image J/FIJI by color deconvolution using RGB vector and binary image conversion.

2.7. Isolation of purified nuclei

Nuclei and post-nuclear supernatant (PNS) were separated as reported elsewhere [25]. All steps were performed at 4°C. Cells were swelled in hypotonic buffer A (10 mM HEPES-KOH, pH 7.9, 1.5 mM $MgCl_2$, 10 mM KCl, 0.5 mM dithiothreitol, 0.05% Nonidet P-40) containing protease inhibitors (Roche), Tenbroeck homogenized, and nuclei were pelleted (220 g, 5 min). Nuclei were washed with buffer A + 0.3% Nonidet P-40 to remove cytoplasmic contaminants and pelleted (600 g, 5 min). Nuclei were resuspended in 0.25 M sucrose/10 mM $MgCl_2$, layered over 0.35 M sucrose/0.5 mM $MgCl_2$ and centrifuged at 1430 g for 5 min. Purified nuclei were stored in buffer B (20 mM HEPES-KOH, pH 7.9, 25% glycerol, 420 mM NaCl, 1.5 mM $MgCl_2$, 0.2 mM EDTA, 0.5 mM DTT, 0.05% Nonidet P-40) containing protease inhibitors. Samples were sonicated using a Branson sonifier (3 × 5 s at 20% output) prior to protein determination by Bradford [48].

2.8. Immunoblotting

SDS-PAGE and immunodetection are described elsewhere [27]. Antibodies: anti-ABCB1 (clone G-1, Santa Cruz or clone C219, Enzo Life Sciences), 1:500; anti-PITX2^{ABC} (Capra Science), 1:2000; anti-lamin A/C (clone 4C11) and anti-GAPDH (clone 14C10) (both Cell Signaling Technology), 1:20,000; anti-histone H1 (clone AE-4, Abcam), 1:500; anti-OCT3, 1:300 (Santa Cruz). Densitometry analyses were performed using FIJI/ImageJ.

2.9. Chromatin immunoprecipitation (ChIP)

Cells at 80–90% confluence in 100 mm dishes were crosslinked with 1% paraformaldehyde/PBS and quenched with 0.125 M glycine. After washing with PBS, harvesting and lysis in 0.25% Triton X-100 buffer, cells were sonicated in SDS lysis buffer (Bioruptor, Diagnode). Precleared lysates were incubated with 4 µg anti-PITX2^{ABC} antibody (Capra Science) or rabbit IgG (Santa Cruz) overnight at 4°C. Antibody-protein complexes were precipitated using protein A magnetic beads (Pierce), eluted and reverse crosslinked at 65°C for 30 min. Protein and RNA were digested with proteinase K (100 µg) and RNase I (50 µg), respectively, at 55°C overnight. DNA was precipitated by phenol-chloroform extraction and resuspended in equal volumes of water.

2.10. Reverse transcriptase semi-quantitative and quantitative real-time PCR

Procedures for semi-quantitative PCR [27] and quantitative PCR (qPCR) [34] have been described elsewhere. Primers for *PITX2* isoforms

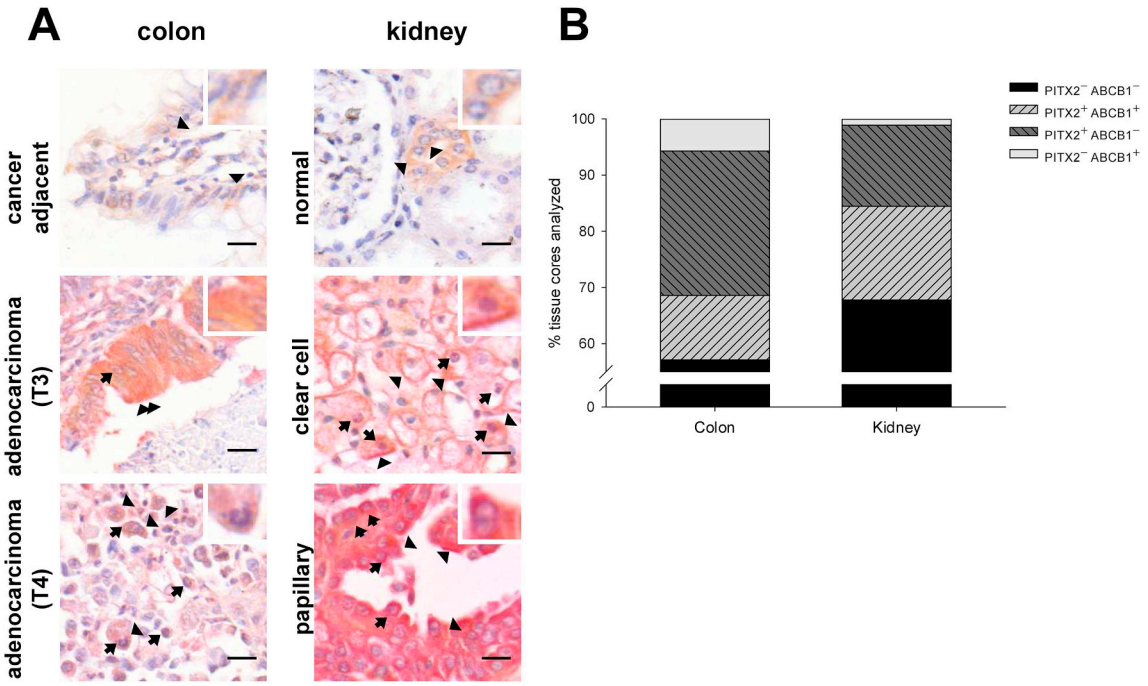

Fig. 2. PITX2-driven ABCB1 expression facilitates drug resistance. (A) Immunohistochemistry of human colon adenocarcinomas and renal carcinomas from TMAs wherein ABCB1 was labeled with 3,3′ diaminobenzidine (DAB, brown) and PITX2 with alkaline phosphatase (AP, red). Nuclei were counterstained with hematoxylin. Images are representative of two independent experiments. Arrows indicate nuclear PITX2 presence, arrowheads indicate ABCB1 expression. Scale bar = 10 µm. (B) Cancer tissue cores (colon, n = 72; kidney, n = 90) were profiled into PITX2 positive only ($PITX2_{nuc}{}^{+}/ABCB1^{-}$), both PITX2 and ABCB1 positive ($PITX2_{nuc}{}^{+}/ABCB1^{+}$), ABCB1 positive only ($PITX2_{nuc}{}^{-}/ABCB1^{+}$) or negative for PITX2 and ABCB1 ($PITX2_{nuc}{}^{-}/ABCB1^{-}$). (C, D) Proportion of tumor cells exhibiting both nuclear PITX2 and ABCB1 ($PITX2_{nuc}{}^{+}/ABCB1^{+}$) or only positive ABCB1 ($PITX2_{nuc}{}^{-}/ABCB1^{+}$) are reported as percentage of total cells. Quantification stems from both immunofluorescence and immunohistochemistry stainings. Five random areas from each core were counted and assessed. An average of 1500 cells was counted per core with a minimum of 500 cells. Statistical analyses using one-way ANOVA compare cancer adjacent normal tissue and cancer subtypes to normal renal or colon tissue. (E) Surface immunostaining for ABCB1 in non-fixed cells. Scale bar = 20 µm. Fluorescence intensity was analyzed by threshold area analysis and normalized to cell number (n = 3). (F) Drug-resistant Colo320DM cells were treated with 0.1 µM PSC833 in serum free medium for 15 min prior to addition of 1 µM doxorubicin (DOX) and incubated for 24 h. Cell viability was assessed by MTT assay (n = 5). One-way ANOVA determined significant differences between groups. (G) *PITX2* mRNA and ABCB1 protein in Colo320DM cells were analyzed by PCR and immunoblotting (IB) after 72 h transient PITX2^{ABC} siRNA transfection. Densitometry analysis of ABCB1 protein reveals significant downregulation by *PITX2*^{ABC} siRNA (n = 4). (H) Clonogenic survival assay of Colo320DM transiently transfected with control or *PITX2*^{ABC} siRNA for 72 h and treated with 1 µM DOX for 24 h. Following detachment, 5000–10,000 cells were replated from single cell suspensions and grown for 7–10 days (n = 5). P-values were derived from unpaired Student's *t*-test (E, G, H). *p < 0.05, **p < 0.01, ***p < 0.001. (For interpretation of the references to color in this figure legend, the reader is referred to the Web version of this article.)

have been previously reported [24]. For ChIP samples, three step cycling was used: activation at 95°C for 5 min followed by 40 cycles of 95°C 30 s, 54.5°C or 57.5°C 30s, 72°C 30 s. Primers spanning putative PITX2 binding sites in drug transporter promoter regions were designed using Primer-BLAST (NCBI) and primer efficiency tests were performed on serially diluted mixed genomic DNAs. Primer sequences are listed in Supplementary Table 2.

2.11. Statistical analyses

Unless otherwise indicated, at least three biological replicates were performed and means ± SE are shown. Statistical analyses were executed using Excel Professional 2010 (Microsoft) or SigmaPlot v12.5 (Systat Software, Inc). Pairwise comparisons employed unpaired Student's t-test. For comparisons of multiple groups, one-way or two-way ANOVA with suitable post-hoc test was used. Statistical significance is reported by $p < 0.05$.

3. Results

3.1. PITX2 is increased in multiple cancers and linked to MDR

From 23 cancers, *PITX2* RNA was elevated in 7 cancers (blood, colon, endometrium, kidney, lung, ovary, uterus) and attenuated in 6 cancers (bladder, breast, esophagus, prostate, skin, vulva) compared to normal tissue (Fig. 1A). Interestingly, cancer types with highest *PITX2* overexpression are intimately linked with intrinsic MDR or MDR development during chemotherapy. We focused on colon cancer, wherein *PITX2* (4.4-fold) is maximally increased, and renal cell carcinoma (RCC) wherein previous studies linked *PITX2* and MDR [27].

Immunofluorescence staining of commercial cancer TMAs confirmed increased nuclear PITX2 ($PITX2_{nuc}$) and percentage of $PITX2_{nuc}^+$ cells in colon adenocarcinomas (Fig. 1C) compared to normal cancer-adjacent tissue. Multiple renal cancer subtypes (clear cell, granular cell, transitional cell, and papillary carcinomas) exhibited up to 50% cells that were $PITX2_{nuc}^+$ (Fig. 1D). Elevated PITX2 was independent of tumor stage, size and extent of primary tumor in mined databases (Fig. 1B) as well as in TMAs (Table 1). Analogous to RCC cells [27], drug-resistant colon adenocarcinoma Colo320DM exhibited augmented $PITX2_{nuc}$ (Fig. 1E), which co-localized with Hoechst DNA stain (Fig. 1F), and translated into enhanced basal *PITX2* promoter activity compared to drug-sensitive Colo205 (Fig. 1G).

PITX2 transcriptionally upregulates MDR P-glycoprotein ABCB1 in drug-resistant RCC cells [27]. Co-staining of PITX2 and ABCB1 in cancer TMAs substantiated our previous findings and indicated higher expression in both kidney and colon (Fig. 2A). Cancer tissue core profiling (72 colon, 90 renal) revealed ~30% of cores exhibited augmented $PITX2_{nuc}^+$ with further classification into: [colon, kidney] $PITX2_{nuc}^+/ABCB1^+$ cores [11.4%, 16.7%] and $PITX2_{nuc}^+/ABCB1^-$ cores [25.7%, 14.4%] (Fig. 2B). Detailed quantification of cell populations within single TMA cores revealed significant increases in % $PITX2_{nuc}^+/ABCB1^+$ cells in RCC (2.1–25.2%), granular cell (4.8–35.5%) and papillary carcinomas (8.9–31.3%) compared to normal and cancer-adjacent tissue whereas no differences were observed for $PITX2_{nuc}^-/ABCB1^+$ cells (Fig. 2D). A large range in both $PITX2_{nuc}^+/ABCB1^+$ and $PITX2_{nuc}^-/ABCB1^+$ cells (0–49.7%) in colon adenocarcinomas was observed (Fig. 2C), however, cores with > 10% $PITX2_{nuc}^+/ABCB1^+$ or $PITX2_{nuc}^-/ABCB1^+$ cells reached statistical significance ($p < 0.025$) over normal tissue.

To ascertain a causal link between PITX2 and ABCB1 in colon

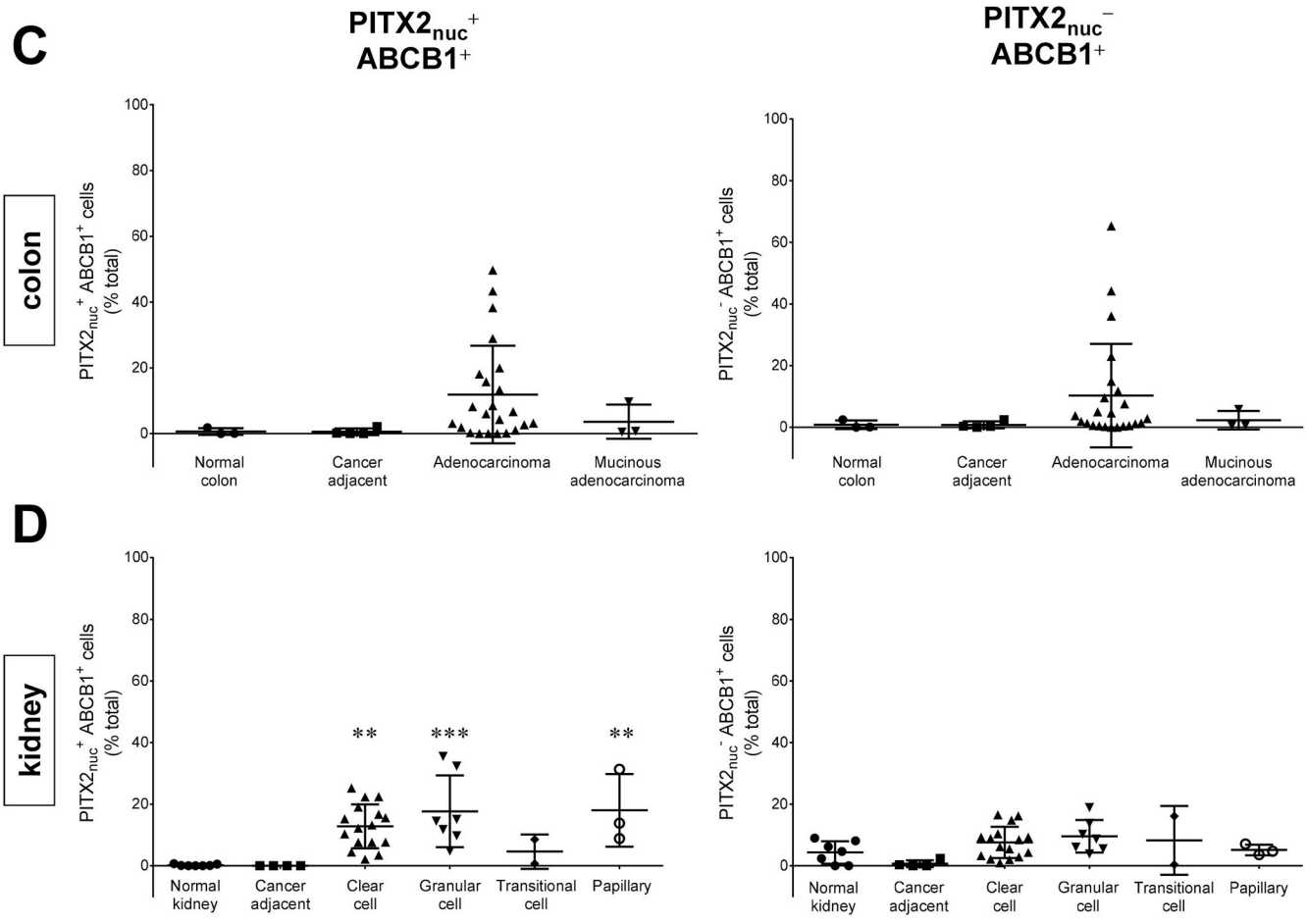

Fig. 2. (*continued*)

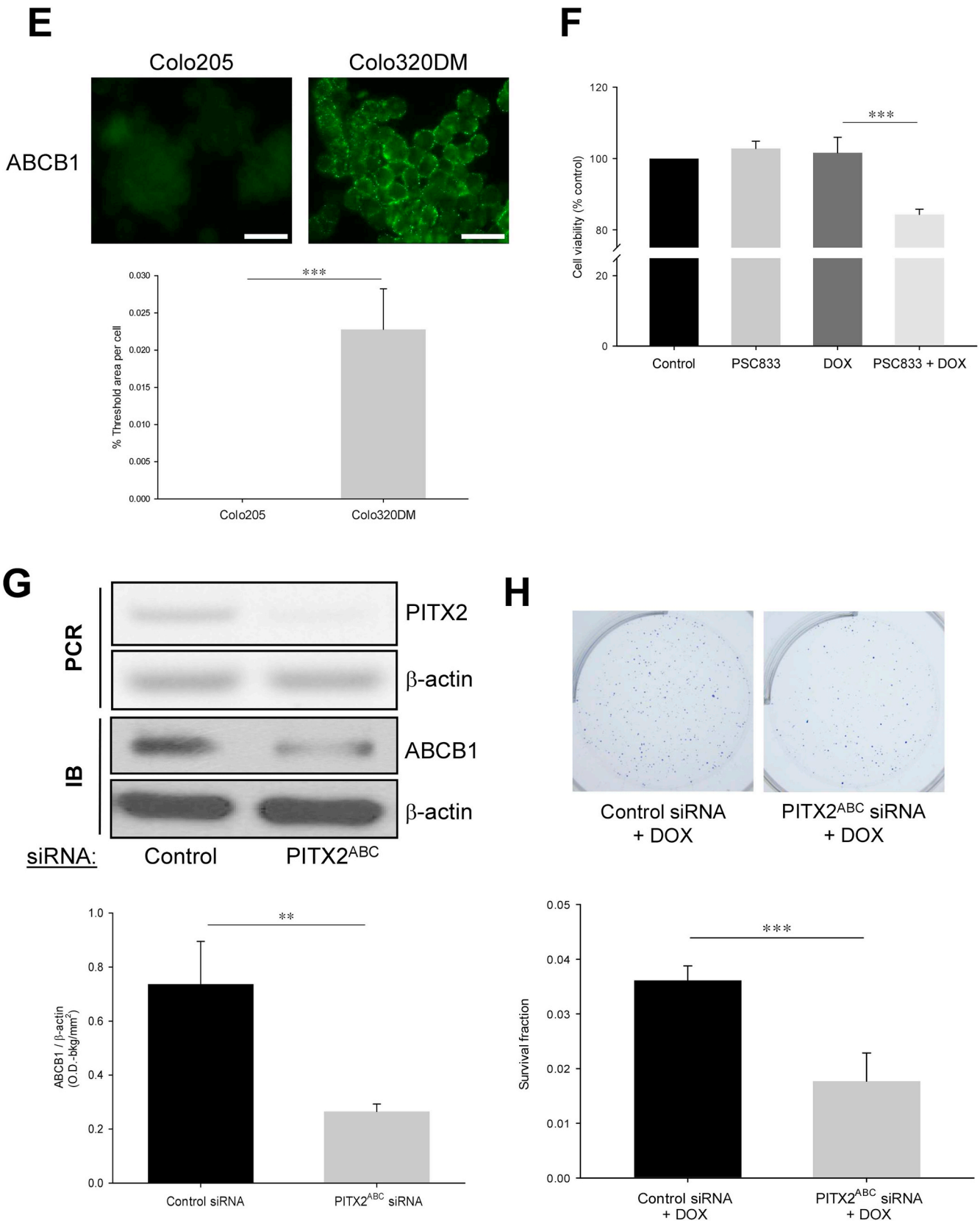

Fig. 2. (*continued*)

cancer, augmented surface ABCB1 (Fig. 2E) and partial reversal in resistance to anthracycline drug and ABCB1 substrate DOX by ABCB1 inhibitor PSC833/valspodar was evidenced in Colo320DM cells (Fig. 2F), which is in line with previous observations in MDR renal cancer A498 cells [27]. *PITX2*^{ABC} siRNA downregulated ABCB1 protein by ~65% (Fig. 2G) and the number of cell colonies after DOX treatment by ~50% in clonogenic survival assays (Fig. 2H). Furthermore, combined *PITX2*^{ABC} siRNA + PSC833 treatment resulted in 7-fold increase

in DOX-induced A498 cell death (Supplementary Fig. 1A).

3.2. Differential regulation of drug transporters by PITX2

ABCB1 was the first molecular link to drug resistance. Since its discovery, other MDR drug transporters, including MRP1/*ABCC1*, BCRP2/*ABCG2* and hOCT3/*SLC22A3*, have been evidenced. We thus explored whether PITX2 facilitates MDR by solely regulating ABCB1 expression or by regulating multiple drug transporters. In Colo320DM, ABCC1 inhibitor MK571 (Fig. 3A) and ABCG2 inhibitor fumitremorgin C (Supplementary Fig. 1B) were ineffective whereas PSC833/valspodar decreased DOX resistance by approximately one-fifth (Fig. 3A). In contrast, A498 DOX resistance (95.8 ± 6.5% cell viability) was attenuated by MK571 (to 61.7 ± 6.1%) or PSC833 (to 73.9 ± 9.1%) (Fig. 3B), indicating both transporters contribute to DOX resistance. PITX2^{ABC} downregulation significantly reduced *ABCB1* and *ABCG2* in Colo320DM (Fig. 3C) or *ABCC1*, *ABCB1* and *ABCG2* in A498 (Fig. 3D). Intriguingly, hOCT3/*SLC22A3* mRNA was increased upon *PITX2*^{ABC} knockdown that was observed for neither hOCT1/*SLC22A1* nor hOCT2/*SLC22A2* (Supplementary Fig. 1C). To better understand the impact of PITX2 on drug import, SW480 cells, which express PITX2$_{nuc}$ (Supplementary Fig. 2A), exhibit enhanced *PITX2* promoter activity (Supplementary Fig. 2B), respond to PITX2^{ABC} siRNA (Supplementary Fig. 2C) and harbor augmented *SLC22A3* mRNA transcripts (SW480 Ct 27.5 versus Colo320DM Ct 32.8), were used to model colon cancer. PITX2 repression of SLC22A3 was verified in immunoblotting experiments in PITX2^{ABC} siRNA-transfected SW480 and A498 (Fig. 3E), resulted in enhanced accumulation of ethidium bromide, an OCT

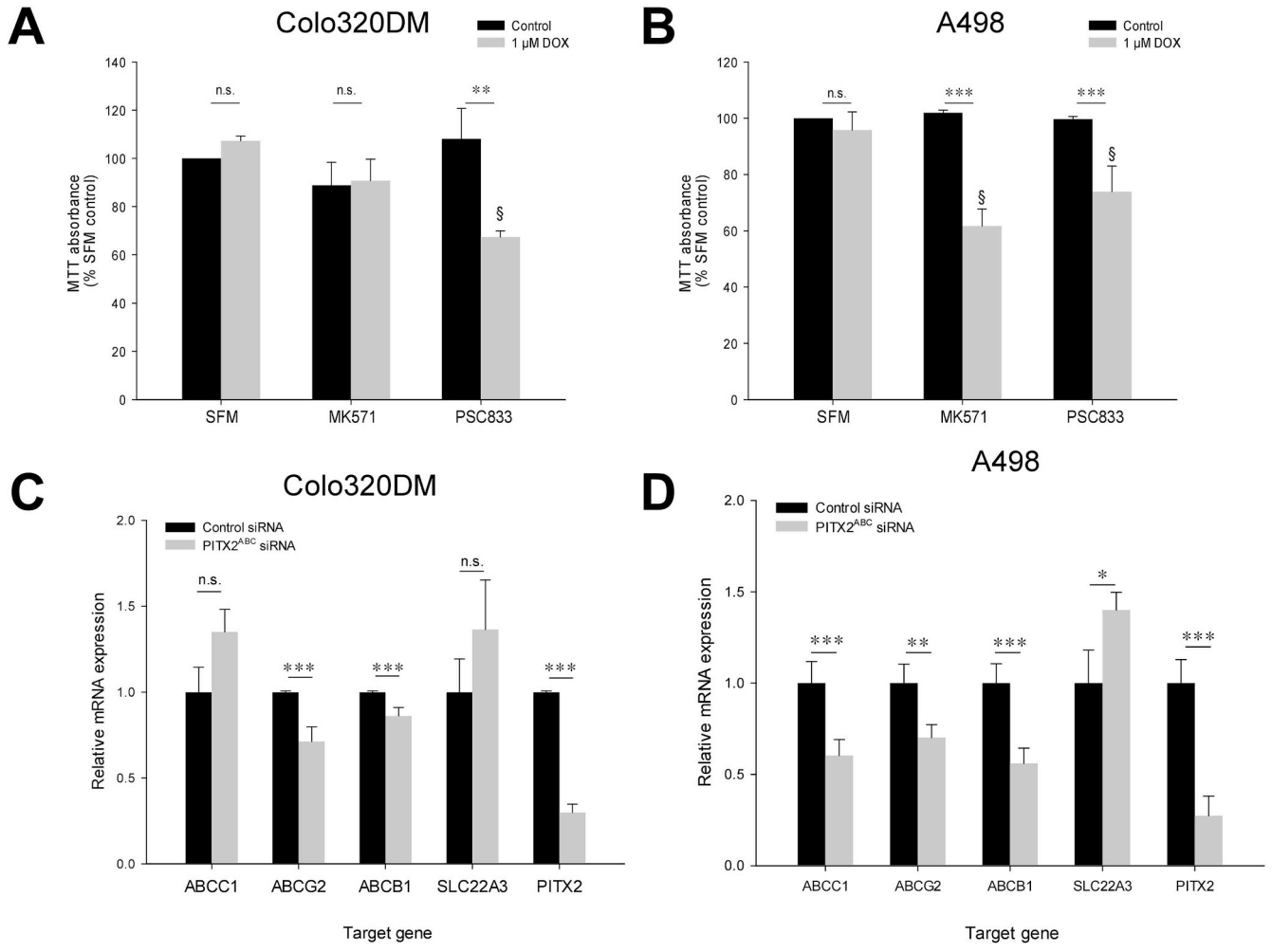

Fig. 3. Differential expression and PITX2-mediated regulation of drug transporters in kidney and colon cancer cell lines. MTT cell viability assay of drug-resistant Colo320DM (A) or A498 (B) cells pretreated with ABCC1 inhibitor MK571 (1 µM for Colo320DM, 10 µM for A498) or ABCB1 inhibitor PSC833 (1 µM) for 30 min and exposed to DOX for 24 h (n = 3). (C, D) Drug transporter mRNA expression was determined by qPCR in drug-resistant cells transfected with PITX2^{ABC} siRNA. Statistical analyses comparing PITX2^{ABC} siRNA to control siRNA were performed using Student's unpaired *t*-test (n = 6–9). Averaged Cq values are as follows: for Colo320DM, ABCC1 22.1, ABCG2 26.5, ABCB1 19.2, SLC22A3 32.2; for A498, ABCC1 22.8, ABCG2 23.4, ABCB1 23.3, SLC22A3, 20.7. (E) SLC22A3 protein was increased in PITX2^{ABC} siRNA transfected drug-resistant cells after 48–72 h. Densitometry analysis was performed on n = 3–10 and statistical significance was reached using Student's unpaired *t*-test. (F) PITX2^{ABC} siRNA-transfected A498 cells were exposed to 10 µg/ml ethidium bromide (EtBr). Intracellular EtBr was determined at each time point (n = 3). Student's unpaired *t*-test compares control to PITX2^{ABC} siRNA. (G) Trypan blue cell viability assay using ABCB1/ABCC1/SLC22A3 substrate vincristine. Cells were transfected with PITX2^{ABC} siRNA for 48 h and subsequently exposed to vincristine (50 nM) in serum-free medium for 24 h (n = 4). Dual regulation of drug exporting transporters and SLC22A3 by PITX2 was expanded to Caco2 colorectal adenocarcinoma, 786-O renal cell adenocarcinoma and Caki-1 clear cell carcinoma cell lines. PITX2^{ABC} siRNA transfected cell lines (25 nM, 72 h) were subjected to qPCR analysis (H) or immunoblot analysis for ABCB1 and SLC22A3 (I). Means ± SE are shown from n = 2–6. (J) Cross-linked chromatin immunoprecipitation (ChIP) with anti-PITX2^{ABC} antibody (4 µg). Semi-quantitative PCR was performed on genomic DNA using primers against putative PITX2 binding sites with 4% input and amplification by 35 cycles. A representative agarose gel is shown for SW480. (K) ChIP samples were subjected to qPCR analysis. Correlation plots reveal PITX2 binding to promoter regions of *ABCB1*, *ABCC1*, *ABCG2* and *SLC22A3*. Data represent two independent experiments. Statistical analyses were performed using one-way ANOVA (A, B) or unpaired Student's *t*-test (C–I) where *p < 0.05, **p < 0.025, ***p < 0.01. (For interpretation of the references to color in this figure legend, the reader is referred to the Web version of this article.)

substrate [28] (Fig. 3F), and augmented cell death by vincristine, which is transported by ABCB1/ABCC1/SLC22A3 [40,41], by 3–5-fold (Fig. 3G).

Our observations of dual regulation of SLC22A3 and ABC drug transporters were extended to additional model cell lines for colon cancer (Caco2) and renal cancer (786-O and Caki-1). Downregulation of PITX2 by $PITX2^{ABC}$ siRNA in Caco2 cells resulted in significantly increased SLC22A3 protein and a tendency towards decreased ABCB1 protein (Fig. 3I) although mRNA transcripts were unchanged (Fig. 3H), suggesting additional posttranscriptional regulation by PITX2. Conversely, the renal cancer cell lines exhibited augmented *SLC22A3* mRNA (786-O, Caki-1) (Fig. 3H) as well as protein (786-O) (Fig. 3I) in $PITX2^{ABC}$ siRNA compared to control siRNA transfected cells. Though ABCB1 mRNA and protein downregulation by $PITX2^{ABC}$ siRNA was evident in Caki-1 cells, ABCB1 was slightly increased in 786-O cells (Fig. 3H and I). Rather, *ABCG2* mRNA was significantly decreased by $PITX2^{ABC}$ siRNA in these cells (Fig. 3H). Interestingly, PITX2 strongly suppressed ABCC1 and ABCG2 in Caki-1 and ABCC1 in Caco2 (Fig. 3H) or Colo320DM (Fig. 3C), indicating PITX2's pivotal role in determining ABC drug transporter expression patterns. These differences may lie in the levels of PITX2 isoforms expressed, accessibility of PITX2 transcription binding sites, and presence of transcriptional blockers that together impact the drug transporter landscape.

We previously identified 2 PITX2 binding sites in the *ABCB1* promoter [27]. Manual sequence analysis of *ABCC1*, *ABCG2* and *SLC22A3* promoter regions (−20 kb) revealed presence of 40, 21 and 9 potential PITX2 binding sites, respectively, for all known consensus sequences (TAATCC, GGATTA, GGCTTAG). Using ChIP, enrichment over control rabbit IgG was observed for all drug transporters when PITX2 was immunoprecipitated (Fig. 3J). Correlation plots of qPCR analysis indicate *PITX2* promoter binding at two putative TAATCC sites for all tested drug transporters in SW480 cells (Fig. 3K). In A498, PITX2 exhibited greater site selectivity, favoring upstream promoter regions of *ABCB1* and *SLC22A3,* and downstream promoter regions of *ABCG2* and *ABCC1* (Fig. 3K).

3.3. All PITX2 isoforms upregulate ABCB1 but cancer cell lines express distinct isoforms

The complex regulatory pattern of drug transporters by PITX2 in A498 cells may be attributed to conglomerate PITX2 isoform expression patterns. PITX2 isoforms and their splice variants [26] are differentially expressed and transcriptionally regulate genes in an isoform-specific manner [5]. *PITX2A* and *PITX2B* mRNA were highly abundant in Colo320DM relative to Colo205 (Fig. 4A) that was confirmed in purified nuclei (Fig. 4B). Conversely, A498 exhibited increased *PITX2C* mRNA only compared to drug-sensitive ACHN renal cancer cells (Fig. 4A), but harbored multiple nuclear PITX2 variants, of which PITX2Cβ was strongly enriched, in purified nuclei (Fig. 4C). Interestingly, PITX2Cα appeared to migrate slower than expected (Fig. 4C, arrowhead) and could represent a highly phosphorylated form. Indeed, tyrosine kinase inhibitor genistein and GSK3 inhibitor SB216763 attenuated PITX2 promoter activity in A498 whereas protein kinase C (PKC) and cyclin-dependent kinase inhibitor UCN-01 had the opposite effect (Fig. 4D). Furthermore, SB216763 partially reversed resistance to DOX (Fig. 4E). Taken together, PITX2 isoform expression appears to be cancer cell-type specific and dependent on its phosphorylation status.

PITX2 isoform expression in non-cancerous HPCT cells with low

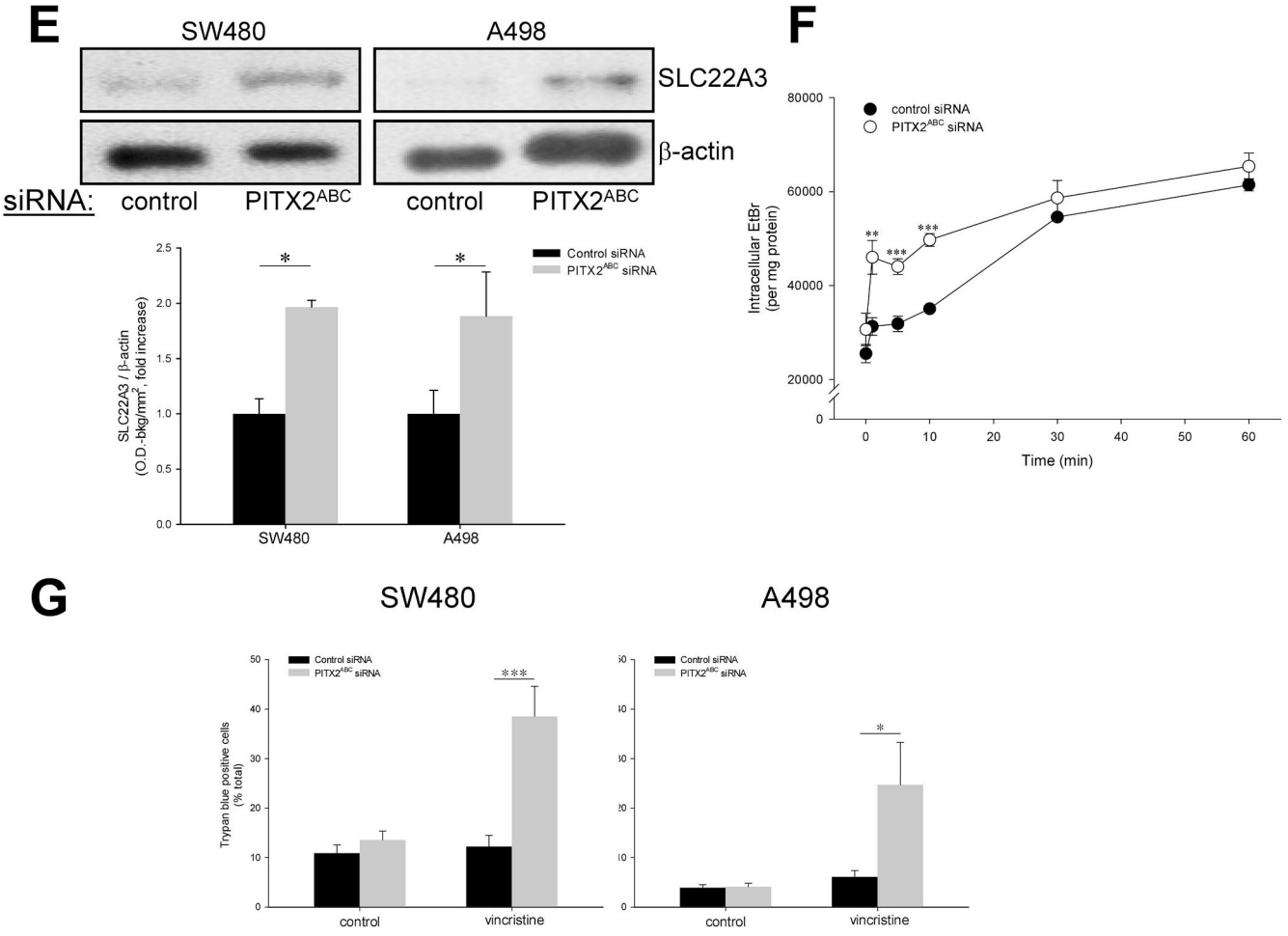

Fig. 3. (*continued*)

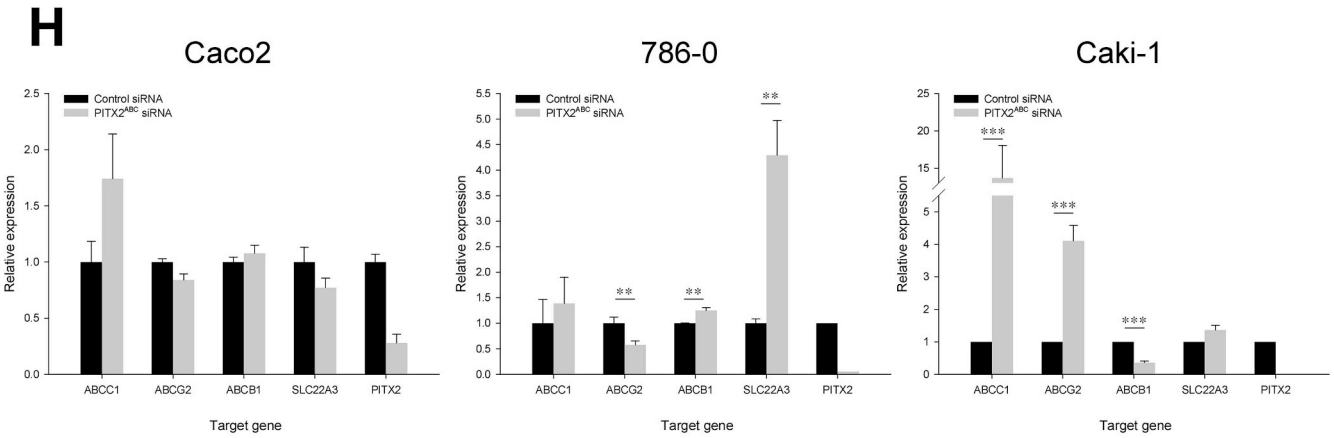

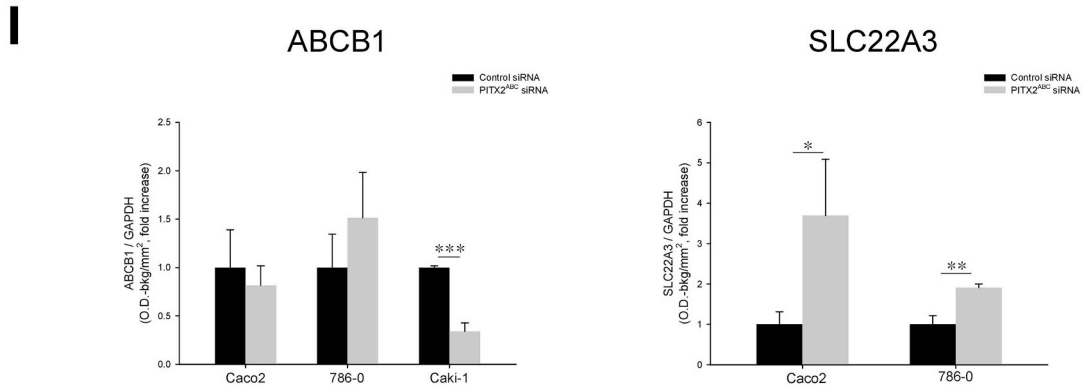

Fig. 3. (*continued*)

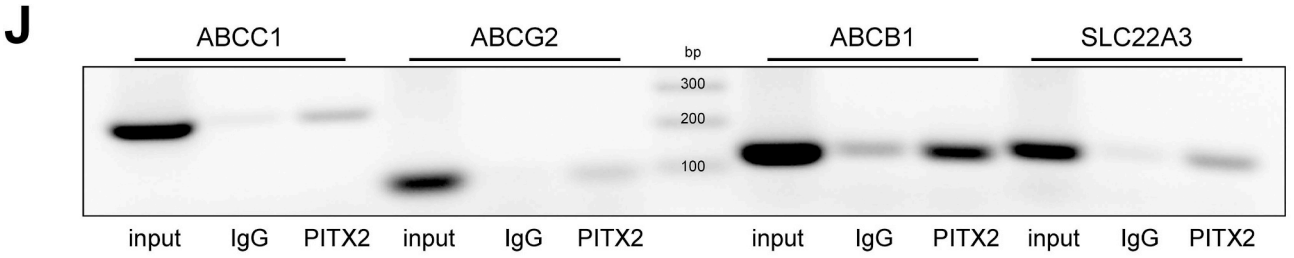

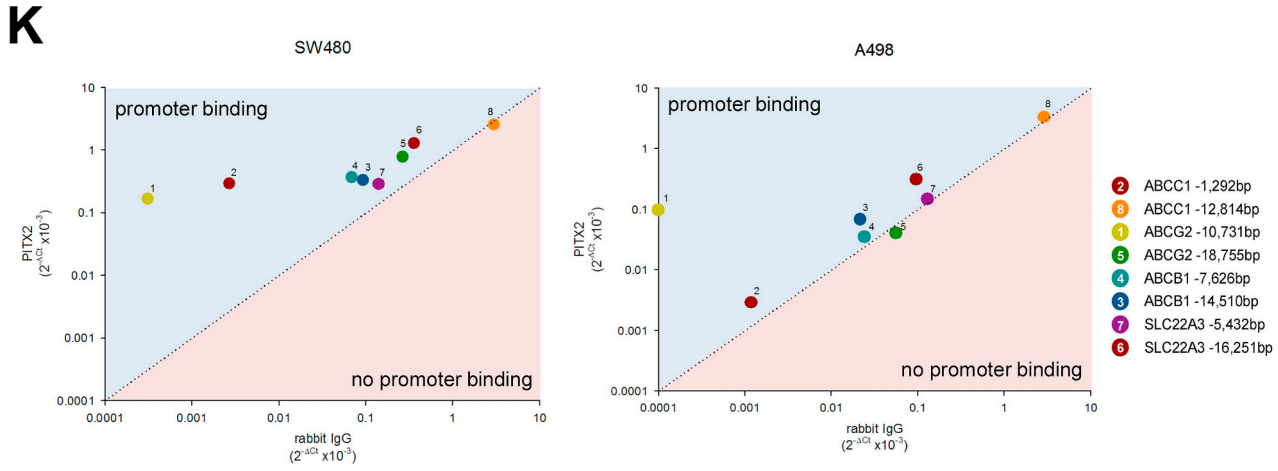

Fig. 3. (*continued*)

ABCB1 resulted in 2.7, 6.7 and 5.9-fold increased ABCB1 by *Pitx2a*, *Pitx2b* and *Pitx2c*, respectively, indicating all *PITX2* isoforms are able to regulate ABCB1 transcription (Fig. 4F). Comparable results were obtained in ACHN (data not shown). Though PITX2 heterodimers can synergistically affect gene expression [5], combined *Pitx2* isoform overexpression did not enhance ABCB1 upregulation compared to single isoform expression in HPCT (Fig. 4G).

In MDR cancer cells, all transcriptional regulatory *Pitx2* isoforms could prevent vincristine cytotoxicity compared to control (EV) (Fig. 4H) whereas only *Pitx2a* and/or *Pitx2c* stimulated proliferation after replating (Fig. 4I). Moreover, *Pitx2c* significantly reduced vincristine-induced cytotoxicity (Fig. 4H) and was the most effective isoform in inversely regulating SLC22A3 and ABCB1 expression in A498 cells (Fig. 4J). To examine the contribution of combined PITX2 isoforms, mild *Pitx2* isoform overexpression in A498 cells to prevent overt cytotoxicity was employed. *Pitx2c* had the largest impact in

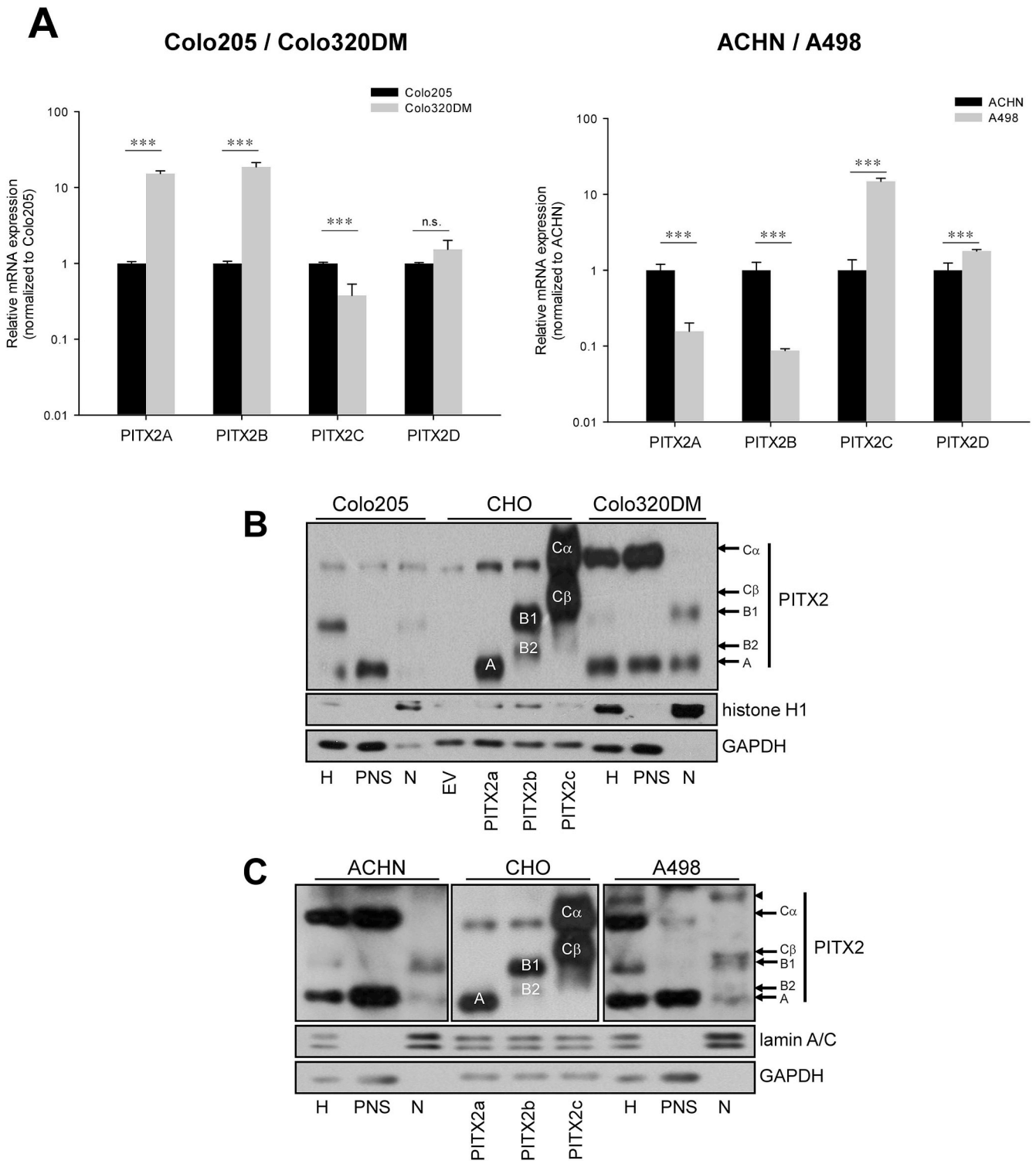

(caption on next page)

Fig. 4. Distinct PITX2 isoform expression is cancer cell type-specific and determines drug transporter landscape. (A) Quantitative real-time PCR analysis of mRNA expression levels of *PITX2* isoforms in human colon (n = 4) and kidney (n = 5) cancer cell lines using β-actin as reference. Pairwise comparisons were performed using unpaired Student's *t*-test . Subcellular fractionation of human colon (B) and kidney (C) cancer cell lines. Purity of fractions was assessed by markers for nucleus (lamin A/C or histone H1) and cytosol (GAPDH). Homogenates of CHO cells overexpressing *mPitx2* isoforms serve as positive controls and were identified on shorter exposed films. Blot is representative of three biological replicates. H, homogenate; PNS, postnuclear supernatant; N, nuclei. (D) PITX2 luciferase assay in A498 exposed to kinase inhibitors. After transfection with PITX2-Luc and Renilla-Luc, A498 cells were treated with tyrosine kinase inhibitor genistein (50 μM), GSK-3 inhibitor SB216763 (1 μM) or protein kinase C and cyclin-dependent kinase inhibitor UCN-01 (0.3 μM) for 12 h, luciferase activity was determined and corrected for Renilla-Luc signals and protein (n = 3). Inhibitor signals were analyzed by one-way ANOVA. (E) MTT assay of A498 cells exposed to 1 μM SB216763 for 48 h and 1 μM DOX in serum-free medium (SFM) for 24 h (n = 4). (F) Densitometry analysis of ABCB1 expression determined by immunoblotting in human renal proximal tubule cells (HPCT) transiently transfected with empty vector (EV) pcDNA3.1 or constructs encoding mouse *Pitx2a*, *Pitx2b* or *Pitx2c* (n = 6). One-way ANOVA compared *Pitx2* isoforms to EV control. (G) *Pitx2* isoforms were singularly or simultaneously expressed using equal amount of plasmid in HPCT cells and analyzed for ABCB1 after 72 h by immunoblotting and densitometry. One-way ANOVA compared PITX2 isoforms to EV (n = 4–7). (H) Colon and kidney cancer cell lines were transfected with low amounts (0.3 μg) of EV or *Pitx2* isoforms for 30 h and treated with 50 nM vincristine in SFM for 24 h. Supernatants and cells were combined and subjected to trypan blue analysis. Percentage trypan blue positive cells is plotted (n = 4–5). Student's unpaired *t*-test compares vincristine to SFM control. (I) Proliferation assay of vincristine-exposed cancer cell lines expressing Pitx2 isoforms. *Pitx2* transient transfection and vincristine treatment was performed as described in (H). 5×10^3 cells were plated in 6-well plates, grown for 7–18 days and fixed and stained. Stained areas were quantified using color deconvolution as described in the Methods and were normalized to EV (n = 4). Representative images are shown from A498 cells. (J) Single PITX2 isoform overexpression in A498 cells. ABCB1 and SLC22A3 were identified by immunoblotting. Image is a representative of n = 3. Relative OD values for target protein/GAPDH are given. (K) Effect of combined *Pitx2* isoforms on drug transporter expression in A498 cells by qPCR 30 h posttransfection (n = 4–5) or (L) immunoblotting 72 h posttransfection (representative blots of n = 4). To avoid cytotoxicity, A498 cells were transiently transfected with 0.1 μg DNA of each isoform plasmid and totaled to 0.3 μg DNA using empty vector (EV). Relative OD values for target protein/GAPDH are given. *p < 0.05, **p < 0.025, ***p < 0.01. (For interpretation of the references to color in this figure legend, the reader is referred to the Web version of this article.)

repressing *SLC22A3* as well as in inducing ABC drug transporter expression, either alone (for *ABCB1*) or in combination with *Pitx2a* (for *ABCC1* and *ABCG2*) (Fig. 4K) and could be recapitulated in immunoblots for ABCB1 and hOCT3/SLC22A3 (Fig. 4L). Furthermore, *Pitx2a* and *Pitx2b* maximally repressed *SLC22A3* and could explain negligible *SLC22A3* in Colo320DM cells, which harbor augmented levels of these PITX2 isoforms (Fig. 4A).

4. Discussion

Here, we demonstrate aberrant PITX2 expression in human cancers and PITX2-dependent transcriptional regulation of drug importers and exporters to confer MDR and enhance cell survival. Drug resistance was maximally reversed by ~50% by *PITX2* downregulation suggesting regulation by additional transcription factors and/or transcription-

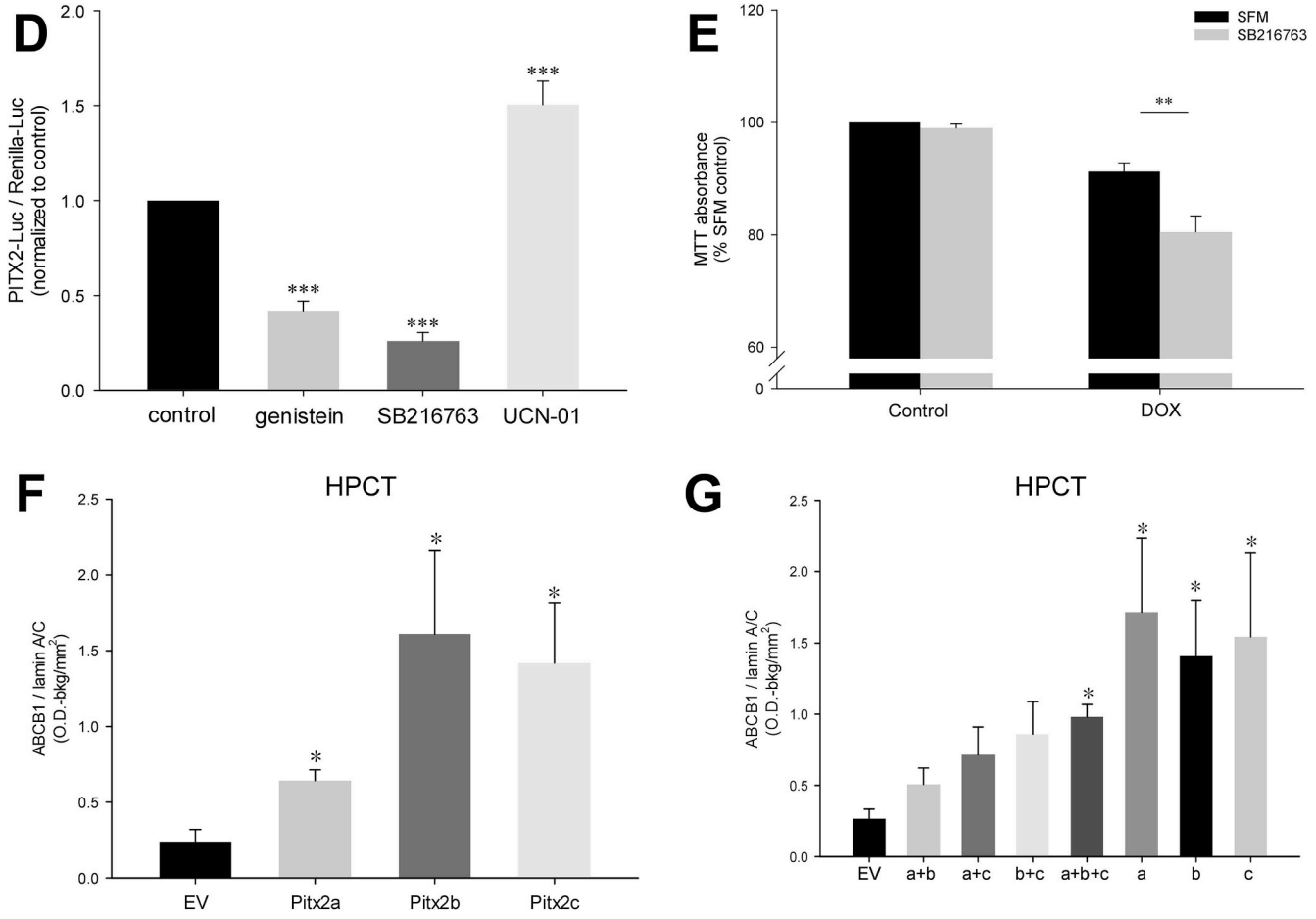

Fig. 4. (*continued*)

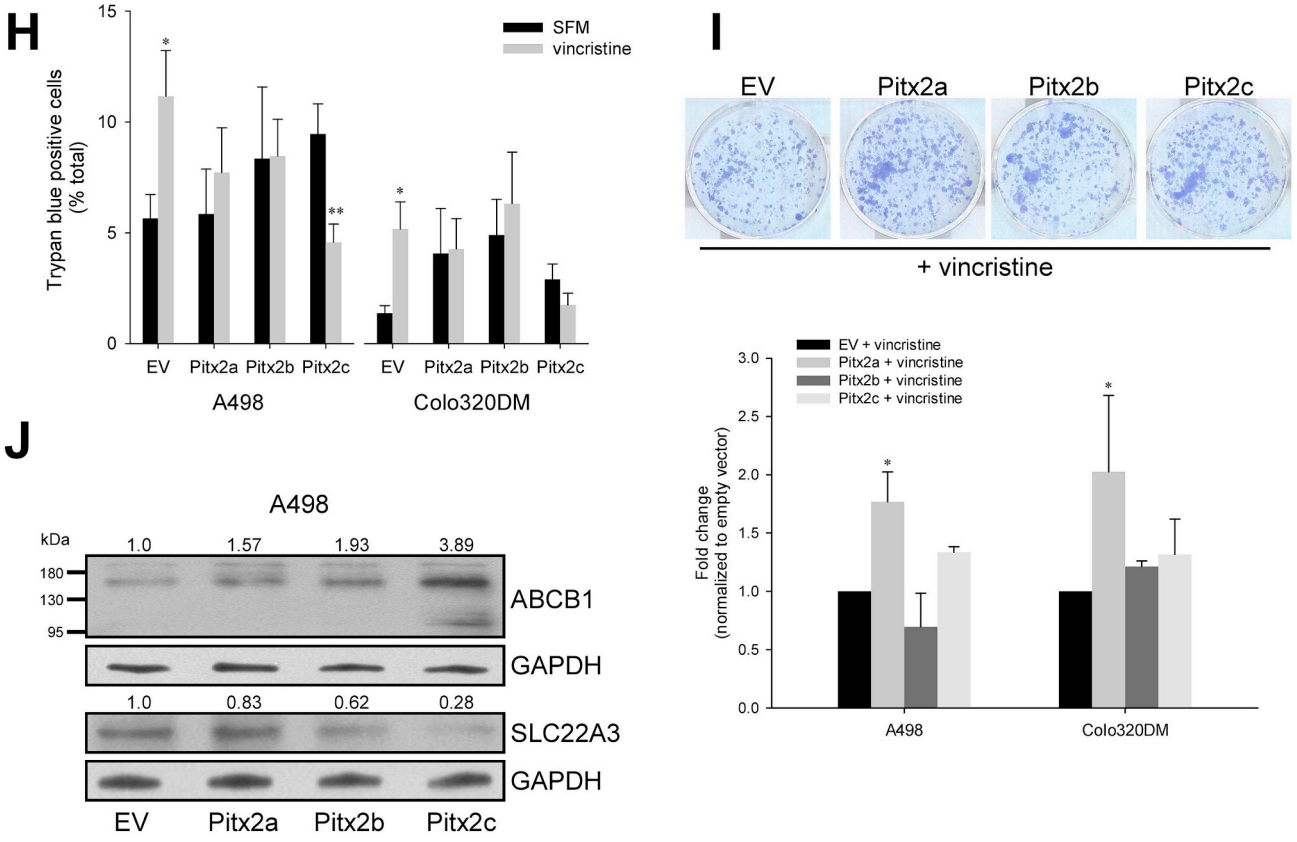

Fig. 4. (*continued*)

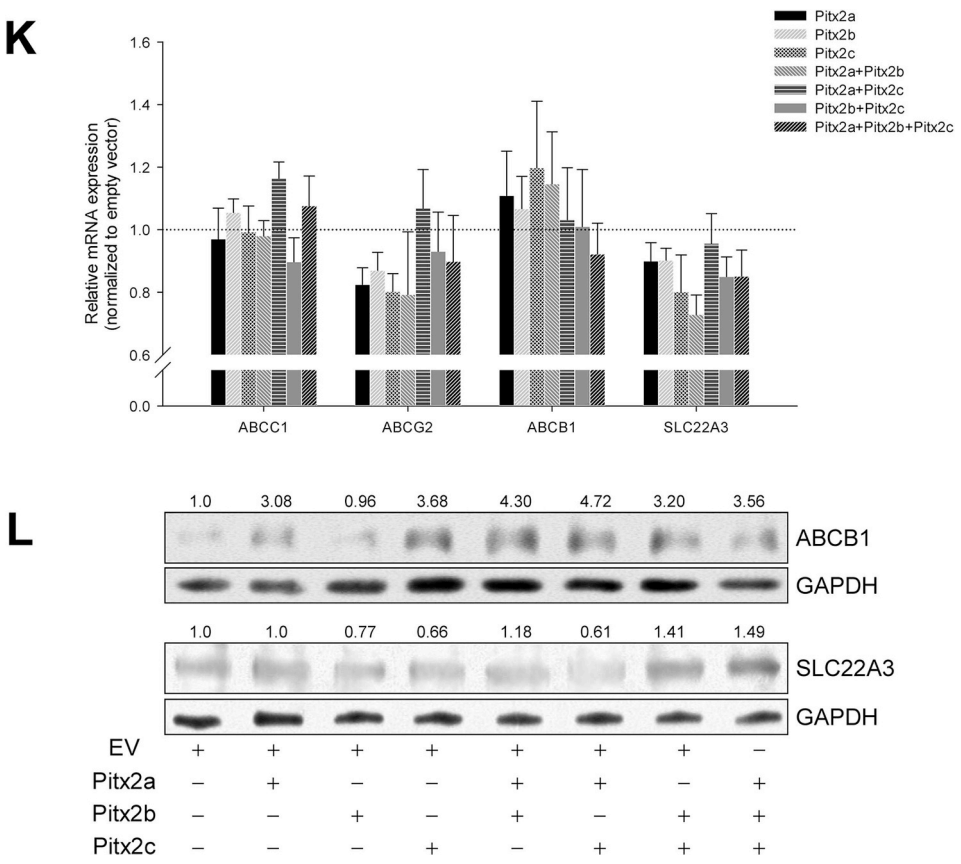

Fig. 4. (*continued*)

independent mechanisms, such as lipid environment. In contrast, ≤10% of cancer TMA cores analyzed exhibited augmented ABCB1 without PITX2 upregulation (Fig. 2B) implying PITX2 is a major ABCB1 regulator in human colon and kidney cancers.

What cellular factors are determinant in aberrant oncogenic PITX2? Maximal *PITX2* RNA changes in patient colon adenocarcinomas (Fig. 1) could possibly be attributed to adenomatous polyposis coli (APC), a negative regulator of β-catenin and frequently mutated in colon cancer, thus driving β-catenin overload and *PITX2* upregulation [23]. In addition, increased PITX2 through microRNAs [6] or tumor-specific DNA hypermethylation [8] of the *PITX2* promoter region were associated with poor outcome and disease progression. Additional potential perturbed mechanisms involved in aberrant oncogenic PITX2 include mRNA export, protein translation and folding, posttranslational modifications, and proteolysis.

PITX2 upregulation appears to be an early event in tumorigenesis occurring at early tumor stages (Fig. 1B, Table 1) thus PITX2 could increase susceptibility or permissibility to manifestation of mutations or adaptive mechanisms by upregulating genes favoring tumor progression, for example, cell cycle control genes [2,11,32], oncogenes [2,11], epithelial-to-mesenchymal (EMT) markers [3], and MDR mediating factors [27]. Alternatively, PITX2 could transcriptionally repress tumor counteracting/suppressor genes or epigenetically alter gene expression [19,33]. The phosphorylation status of PITX2 is critical for its function [9] (Fig. 4D). Although PITX2 is a target gene of Wnt/β-catenin [23], which is regulated by GSK3β phosphorylation of β-catenin resulting in its destruction, our observations indicate Wnt/β-catenin-independent regulation of PITX2 by GSK3: 1) PITX2 promoter activity does not increase upon GSK3 inhibition (which would stabilize β-catenin); 2) transcriptional regulation of ABCB1 by PITX2 functions in β-catenin-deficient cells [27]; 3) putative GSK3 phosphorylation sites are present in PITX2 (isoform C > A = B). GSK3 phosphorylation of PITX2 may affect its DNA binding capacity, analogous to PKC phosphorylation [9], rather than cytoplasmic-to-nucleus shuttling since GSK3 inhibition did not affect nuclear PITX2 localization (data not shown).

Despite the strong link between PITX2 and cancer, endogenous isoform-specific expression has not yet been described. Here, we report for the first time that nuclear PITX2 isoforms are dependent on neoplastic tissue origin forming distinct expression patterns (Fig. 4). Synergistic potential of multiple PITX2 isoforms predicts amplified PITX2 activity in A498, which express several PITX2 variants. In fact, *PITX2* reporter gene activity reveals ~5-fold difference: 1.06 ± 0.81 arbitrary units, n = 4 in A498 [27] versus 0.21 ± 0.25 arbitrary units, n = 9 in Colo320DM (this report); $p < 0.01$. Specific gene subsets are regulated by each PITX2 isoform during embryonic development and seem applicable to oncogenic PITX2. Ectopic *PITX2A*, *PITX2B* or *PITX2C* overexpression in ovarian cancer cell lines activated TGFβ signaling and promoted invasion as well as EMT, but with *PITX2* isoform gene activation selectivity [3]. Selective repression of hOCT3/SLC22A3 (Supplementary Fig. 1C) as well as heterogeneous positive and negative regulation of ABC transporters (Fig. 3) affirms specificity of PITX2 on select MDR genes. The data in Fig. 4 suggest PITX2C, and to a lesser extent PITX2A, is paramount to MDR of kidney cancer cells whereas PITX2A is relevant for colon cancer cells. The role of PITX2B, which despite nuclear presence was ineffective in promoting proliferation after vincristine, is unclear. *PITX2D* mRNA was slightly increased in MDR cells (Fig. 4A) and could be central to determining which isoforms are transcriptionally active through negative regulation [5].

The challenge of eradicating MDR cancers lies not only in unresponsive tumor cells but also encompasses tenacity of cancer stem cells (CSC) [7] and persister cancer cells [36] that are drug-tolerant and contribute to tumor repopulation and persistence, respectively. CSCs express multiple ABC drug transporters whereas persister cancer cells harbor reversible MDR without altered drug transporter expression, which is linked to ferroptosis evasion [16]. Intriguingly, persister cancer cells express augmented stemness marker CD44 [16]. Since PITX2 belongs to the evolutionarily conserved HOX gene family, which has been linked to CD44 expression, EMT, and inverse regulation of drug importers and exporters from this study, it remains to be seen whether PITX2 has a role in conferring tumor persistence to bestow enhanced tumor cell survival and metastatic potential.

Competing interests

The authors declare that they have no competing interests.

Authors' contributions

W.K.L. conceived the study design, performed experiments, analyzed and interpreted data, and wrote the manuscript. F.T. conceived the study design, interpreted data and wrote the manuscript.

Conflicts of interest

None.

Funding

This work was supported by the Intramural Research Program of Witten/Herdecke University (IFF2016-20 to W.K.L), Westermann-Westerdorp Foundation (to W.K.L.) and by the Deutsche Forschungsgemeinschaft (TH345/10-1 to F.T.).

Acknowledgements

We would like to acknowledge Mrs. Bettina Scharner for expert technical assistance and Dr. Claudia Hagedorn for expert advice and technical support in chromatin immunoprecipitation experiments.

Appendix A. Supplementary data

Supplementary data to this article can be found online at https://doi.org/10.1016/j.canlet.2019.01.044.

References

[1] S.G. Aller, J. Yu, A. Ward, Y. Weng, S. Chittaboina, R. Zhuo, P.M. Harrell, Y.T. Trinh, Q. Zhang, I.L. Urbatsch, G. Chang, Structure of P-glycoprotein reveals a molecular basis for poly-specific drug binding, Science 323 (2009) 1718–1722.
[2] S.H. Baek, C. Kioussi, P. Briata, D. Wang, H.D. Nguyen, K.A. Ohgi, C.K. Glass, A. Wynshaw-Boris, D.W. Rose, M.G. Rosenfeld, Regulated subset of G1 growth-control genes in response to derepression by the Wnt pathway, Proc. Natl. Acad. Sci. U. S. A. 100 (2003) 3245–3250.
[3] M. Basu, R. Bhattacharya, U. Ray, S. Mukhopadhyay, U. Chatterjee, S.S. Roy, Invasion of ovarian cancer cells is induced by PITX2-mediated activation of TGF-beta and Activin-A, Mol. Cancer 14 (2015) 162.
[4] M.A. Charles, H. Suh, T.A. Hjalt, J. Drouin, S.A. Camper, P.J. Gage, PITX genes are required for cell survival and Lhx3 activation, Mol. Endocrinol. 19 (2005) 1893–1903.
[5] C.J. Cox, H.M. Espinoza, B. McWilliams, K. Chappell, L. Morton, T.A. Hjalt, E.V. Semina, B.A. Amendt, Differential regulation of gene expression by PITX2 isoforms, J. Biol. Chem. 277 (2002) 25001–25010.
[6] M. Cui, M. Zhang, H.F. Liu, J.P. Wang, Effects of microRNA-21 targeting PITX2 on proliferation and apoptosis of pituitary tumor cells, Eur. Rev. Med. Pharmacol. Sci. 21 (2017) 2995–3004.
[7] M. Dean, T. Fojo, S. Bates, Tumour stem cells and drug resistance, Nat. Rev. Cancer 5 (2005) 275–284.
[8] D. Dietrich, O. Hasinger, V. Liebenberg, J.K. Field, G. Kristiansen, A. Soltermann, DNA methylation of the homeobox genes PITX2 and SHOX2 predicts outcome in non-small-cell lung cancer patients, Am. J. Surg. Pathol. 21 (2012) 93–104.
[9] H.M. Espinoza, M. Ganga, U. Vadlamudi, D.M. Martin, B.P. Brooks, E.V. Semina, J.C. Murray, B.A. Amendt, Protein kinase C phosphorylation modulates N- and C-terminal regulatory activities of the PITX2 homeodomain protein, Biochemistry 44 (2005) 3942–3954.
[10] L. Fu, Y.R. Qin, X.Y. Ming, X.B. Zuo, Y.W. Diao, L.Y. Zhang, J. Ai, B.L. Liu, T.X. Huang, T.T. Cao, B.B. Tan, D. Xiang, C.M. Zeng, J. Gong, Q. Zhang, S.S. Dong, J. Chen, H. Liu, J.L. Wu, R.Z. Qi, D. Xie, L.D. Wang, X.Y. Guan, RNA editing of SLC22A3 drives early tumor invasion and metastasis in familial esophageal cancer,

Proc. Natl. Acad. Sci. U. S. A. 114 (2017) E4631–E4640.
[11] F.K. Fung, D.W. Chan, V.W. Liu, T.H. Leung, A.N. Cheung, H.Y. Ngan, Increased expression of PITX2 transcription factor contributes to ovarian cancer progression, PLoS One 7 (2012) e37076.
[12] P.J. Gage, H. Suh, S.A. Camper, The bicoid-related Pitx gene family in development, Mamm. Genome 10 (1999) 197–200.
[13] M. Ganga, H.M. Espinoza, C.J. Cox, L. Morton, T.A. Hjalt, Y. Lee, B.A. Amendt, PITX2 isoform-specific regulation of atrial natriuretic factor expression: synergism and repression with Nkx2.5, J. Biol. Chem. 278 (2003) 22437–22445.
[14] M.M. Gottesman, T. Fojo, S.E. Bates, Multidrug resistance in cancer: role of ATP-dependent transporters, Nat. Rev. Cancer 2 (2002) 48–58.
[15] C. Grisanzio, L. Werner, D. Takeda, B.C. Awoyemi, M.M. Pomerantz, H. Yamada, P. Sooriakumaran, B.D. Robinson, R. Leung, A.C. Schinzel, I. Mills, H. Ross-Adams, D.E. Neal, M. Kido, T. Yamamoto, G. Petrozziello, E.C. Stack, R. Lis, P.W. Kantoff, M. Loda, O. Sartor, S. Egawa, A.K. Tewari, W.C. Hahn, M.L. Freedman, Genetic and functional analyses implicate the NUDT11, HNF1B, and SLC22A3 genes in prostate cancer pathogenesis, Proc. Natl. Acad. Sci. U. S. A. 109 (2012) 11252–11257.
[16] M.J. Hangauer, V.S. Viswanathan, M.J. Ryan, D. Bole, J.K. Eaton, A. Matov, J. Galeas, H.D. Dhruv, M.E. Berens, S.L. Schreiber, F. McCormick, M.T. McManus, Drug-tolerant persister cancer cells are vulnerable to GPX4 inhibition, Nature 551 (2017) 247–250.
[17] M. Heise, A. Lautem, J. Knapstein, J.M. Schattenberg, M. Hoppe-Lotichius, D. Foltys, N. Weiler, A. Zimmermann, A. Schad, D. Grundemann, G. Otto, P.R. Galle, M. Schuchmann, T. Zimmermann, Downregulation of organic cation transporters OCT1 (SLC22A1) and OCT3 (SLC22A3) in human hepatocellular carcinoma and their prognostic significance, BMC Cancer 12 (2012) 109.
[18] F. Hernandez-Torres, D. Franco, A.E. Aranega, F. Navarro, Expression patterns and immunohistochemical localization of PITX2B transcription factor in the developing mouse heart, Int. J. Dev. Biol. 59 (2015) 247–254.
[19] T. Hilton, M.K. Gross, C. Kioussi, Pitx2-dependent occupancy by histone deacetylases is associated with T-box gene regulation in mammalian abdominal tissue, J. Biol. Chem. 285 (2010) 11129–11142.
[20] H. Hirose, H. Ishii, K. Mimori, F. Tanaka, I. Takemasa, T. Mizushima, M. Ikeda, H. Yamamoto, M. Sekimoto, Y. Doki, M. Mori, The significance of PITX2 overexpression in human colorectal cancer, Ann. Surg. Oncol. 18 (2011) 3005–3012.
[21] C.M. Hsu, P.M. Lin, J.G. Chang, H.C. Lin, S.H. Li, S.F. Lin, M.Y. Yang, Upregulated SLC22A3 has a potential for improving survival of patients with head and neck squamous cell carcinoma receiving cisplatin treatment, Oncotarget 8 (2017) 74348–74358.
[22] Y. Huang, C.J. Guigon, J. Fan, S.Y. Cheng, G.Z. Zhu, Pituitary homeobox 2 (PITX2) promotes thyroid carcinogenesis by activation of cyclin D2, Cell Cycle 9 (2010) 1333–1341.
[23] C. Kioussi, P. Briata, S.H. Baek, D.W. Rose, N.S. Hamblet, T. Herman, K.A. Ohgi, C. Lin, A. Gleiberman, J. Wang, V. Brault, P. Ruiz-Lozano, H.D. Nguyen, R. Kemler, C.K. Glass, A. Wynshaw-Boris, M.G. Rosenfeld, Identification of a Wnt/Dvl/beta-Catenin– > Pitx2 pathway mediating cell-type-specific proliferation during development, Cell 111 (2002) 673–685.
[24] P. Kirchhof, P.C. Kahr, S. Kaese, I. Piccini, I. Vokshi, H.H. Scheld, H. Rotering, L. Fortmueller, S. Laakmann, S. Verheule, U. Schotten, L. Fabritz, N.A. Brown, PITX2c is expressed in the adult left atrium, and reducing Pitx2c expression promotes atrial fibrillation inducibility and complex changes in gene expression, Circ. Cardio. Genet. 4 (2011) 123–133.
[25] Y.W. Lam, A.I. Lamond, Isolation of Nucleoli, in: J.E. Celis (Ed.), Cell Biology: A Laboratory Handbook, Elsevier Academic Press, Burlington, MA, 2006, pp. 103–108.
[26] P. Lamba, T.A. Hjalt, D.J. Bernard, Novel forms of Paired-like homeodomain transcription factor 2 (PITX2): generation by alternative translation initiation and mRNA splicing, *BMC*, Mol. Biol. 9 (2008) 31.
[27] W.K. Lee, P.K. Chakraborty, F. Thévenod, Pituitary homeobox 2 (PITX2) protects renal cancer cell lines against doxorubicin toxicity by transcriptional activation of the multidrug transporter ABCB1, Int. J. Cancer 133 (2013) 556–567.
[28] W.K. Lee, M. Reichold, B. Edemir, G. Ciarimboli, R. Warth, H. Koepsell, F. Thévenod, Organic cation transporters OCT1, 2, and 3 mediate high-affinity transport of the mutagenic vital dye ethidium in the kidney proximal tubule, Am. J. Physiol. Renal. Physiol. 296 (2009) F1504–F1513.
[29] G.D. Leonard, T. Fojo, S.E. Bates, The role of ABC transporters in clinical practice, Oncologist 8 (2003) 411–424.
[30] C.R. Lin, C. Kioussi, S. O'Connell, P. Briata, D. Szeto, F. Liu, J.C. Izpisua-Belmonte, M.G. Rosenfeld, Pitx2 regulates lung asymmetry, cardiac positioning and pituitary and tooth morphogenesis, Nature 401 (1999) 279–282.
[31] Y. Liu, Y. Huang, G.Z. Zhu, Cyclin A1 is a transcriptional target of PITX2 and overexpressed in papillary thyroid carcinoma, Mol. Cell. Biochem. 384 (2013) 221–227.
[32] E. Lozano-Velasco, D. Vallejo, F.J. Esteban, C. Doherty, F. Hernandez-Torres, D. Franco, A.E. Aranega, A pitx2-MicroRNA pathway modulates cell proliferation in myoblasts and skeletal-muscle satellite cells and promotes their commitment to a myogenic cell fate, Mol. Cell Biol. 35 (2015) 2892–2909.
[33] T. Mikeska, C. Bock, H. Do, A. Dobrovic, DNA methylation biomarkers in cancer: progress towards clinical implementation, Expert Rev. Mol. Diagn. 12 (2012) 473–487.
[34] A.R. Nair, K. Smeets, E. Keunen, W.K. Lee, F. Thevenod, E. Van Kerkhove, A. Cuypers, Renal cells exposed to cadmium in vitro and in vivo: normalizing gene expression data, J. Appl. Toxicol. 35 (2015) 478–484.
[35] D.E. Orosz, P.G. Woost, R.J. Kolb, M.B. Finesilver, W. Jin, P.S. Frisa, C.K. Choo, C.F. Yau, K.W. Chan, M.I. Resnick, J.G. Douglas, J.C. Edwards, J.W. Jacobberger, U. Hopfer, Growth, immortalization, and differentiation potential of normal adult human proximal tubule cells, In Vitro Cell. Dev. Biol. Anim. 40 (2004) 22–34.
[36] M. Ramirez, S. Rajaram, R.J. Steininger, D. Osipchuk, M.A. Roth, L.S. Morinishi, L. Evans, W. Ji, C.H. Hsu, K. Thurley, S. Wei, A. Zhou, P.R. Koduru, B.A. Posner, L.F. Wu, S.J. Altschuler, Diverse drug-resistance mechanisms can emerge from drug-tolerant cancer persister cells, Nat. Commun. 7 (2016) 10690.
[37] J. Schindelin, I. Arganda-Carreras, E. Frise, V. Kaynig, M. Longair, T. Pietzsch, S. Preibisch, C. Rueden, S. Saalfeld, B. Schmid, J.Y. Tinevez, D.J. White, V. Hartenstein, K. Eliceiri, P. Tomancak, A. Cardona, Fiji: an open-source platform for biological-image analysis, Nat. Methods 9 (2012) 676–682.
[38] K.W. Scotto, Transcriptional regulation of ABC drug transporters, Oncogene 22 (2003) 7496–7511.
[39] G. Shin, T.W. Kang, S. Yang, S.J. Baek, Y.S. Jeong, S.Y. Kim, GENT: gene expression database of normal and tumor tissues, Cancer Inform. 10 (2011) 149–157.
[40] V. Shnitsar, R. Eckardt, S. Gupta, J. Grottker, G.A. Muller, H. Koepsell, G. Burckhardt, Y. Hagos, Expression of human organic cation transporter 3 in kidney carcinoma cell lines increases chemosensitivity to melphalan, irinotecan, and vincristine, Cancer Res. 69 (2009) 1494–1501.
[41] G. Szakacs, J.K. Paterson, J.A. Ludwig, C. Booth-Genthe, M.M. Gottesman, Targeting multidrug resistance in cancer, Nat. Rev. Drug Dis. 5 (2006) 219–234.
[42] N. Takebe, L. Miele, P.J. Harris, W. Jeong, H. Bando, M. Kahn, S.X. Yang, S.P. Ivy, Targeting Notch, Hedgehog, and Wnt pathways in cancer stem cells: clinical update, Nat. Rev. Clin. Oncol. 12 (2015) 445–464.
[43] G. Tao, P.C. Kahr, Y. Morikawa, M. Zhang, M. Rahmani, T.R. Heallen, L. Li, Z. Sun, E.N. Olson, B.A. Amendt, J.F. Martin, Pitx2 promotes heart repair by activating the antioxidant response after cardiac injury, Nature 534 (2016) 119–123.
[44] Q. Wang, J. Li, W. Wu, R. Shen, H. Jiang, Y. Qian, Y. Tang, T. Bai, S. Wu, L. Wei, Y. Zang, J. Zhang, L. Wang, Smad4-dependent suppressor pituitary homeobox 2 promotes PPP2R2A-mediated inhibition of Akt pathway in pancreatic cancer, Oncotarget 7 (2016) 11208–11222.
[45] Q. Wei, Pitx2a binds to human papillomavirus type 18 E6 protein and inhibits E6-mediated P53 degradation in HeLa cells, J. Biol. Chem. 280 (2005) 37790–37797.
[46] Q. Wei, R.S. Adelstein, Pitx2a expression alters actin-myosin cytoskeleton and migration of HeLa cells through Rho GTPase signaling, Mol. Biol. Cell 13 (2002) 683–697.
[47] T. Yamagishi, S. Sahni, D.M. Sharp, A. Arvind, P.J. Jansson, D.R. Richardson, P-glycoprotein mediates drug resistance via a novel mechanism involving lysosomal sequestration, J. Biol. Chem. 288 (2013) 31761–31771.
[48] M.M. Bradford, A rapid and sensitive method for the quantitation of microgram quantities of protein utilizing the principle of protein-dye binding, Anal. Chem 7 (1976) 248–254.